Unsaturated Zone Hydrology for Scientists and Engineers

James A. Tindall, Ph.D.

United States Geological Survey, National Research Program
Department of Geography and Environmental Sciences, University of Colorado Denver

James R. Kunkel, Ph.D., P.E.

Knight Piésold, LLC, Denver, Colorado;
Department of Geology and Geological Engineering, Colorado School of Mines

with

Dean E. Anderson, Ph.D.

United States Geological Survey, National Research Program

PRENTICE HALL
Upper Saddle River, New Jersey 07458

3

Behavior of Clay–Water Systems

INTRODUCTION

Dispersion and flocculation play an important role in determining the physical and chemical behavior of soil colloidal fractions. This is particularly true in the areas of colloidal facilitated transport, crusting, infiltration, cracking, and swelling (Aly and Letey 1988; Babcock 1963; Goldberg and Forster 1990).

The process of dispersion and flocculation can be understood as occurring in four stages. Stage I is the dry state of the soil. We assume that the initial dry aggregate contains clay particles, which have their own forces of attraction. When this aggregate is "wetted up," the reactions due to hydration separate the individual particles; the distance of separation depends on the number of water molecules bound between cations and the clay surface to which they are attracted.

The process by which the particles are hydrated and pushed apart is known as stage II, or the swelling/slaking stage. Monovalent cations are normally bound ionically, whereas divalent ions such as calcium and magnesium are typically bound to the clay particle by polar covalent bonds. Increases in ionic bonding cause hydration and, thus, soil swelling. When polar covalent bonding is dominant, hydration is limited; generally, only crystalline swelling occurs. Such is the case with calcium clays, which can be dispersed when the soil water content is high and an external mechanical stress is applied.

When sufficient water has been added that the clay particles are separated by a distance of approximately 7 nm, the cations are no longer linked to the clay particle surface, because the cationic charge is shielded by water molecules. The clay is then completely dispersed, and stage III has been reached. Repulsive forces dominate; the repulsive forces are proportional to the charge of the individual clay particle. It is only at this stage that the DLVO theory (explained in section 3.3) is applicable.

Once a system is dispersed in stage III, it can become dehydrated and flocculated, reaching stage IV. Although both divalent and monovalent clays can exist in dispersive conditions, the reformation of polar covalent bonding can occur in divalent cationic clay systems. Such a process will normally be assisted by dehydration due to osmotic effects (salts present in solution). As a result, flocculation occurs due to the combined effects of the nature of bonding in the system (ion type, charge, and concentration) and of dehydration. The type of bonding that occurs depends primarily on the charge structure of the cations present.

In summary, hydration occurs between stage I and stage II, and swelling or slaking of the system has occurred at the attainment of stage II. For typical clay systems, mechanical separation occurs from stage II to stage III, and when stage III is reached, dispersion has

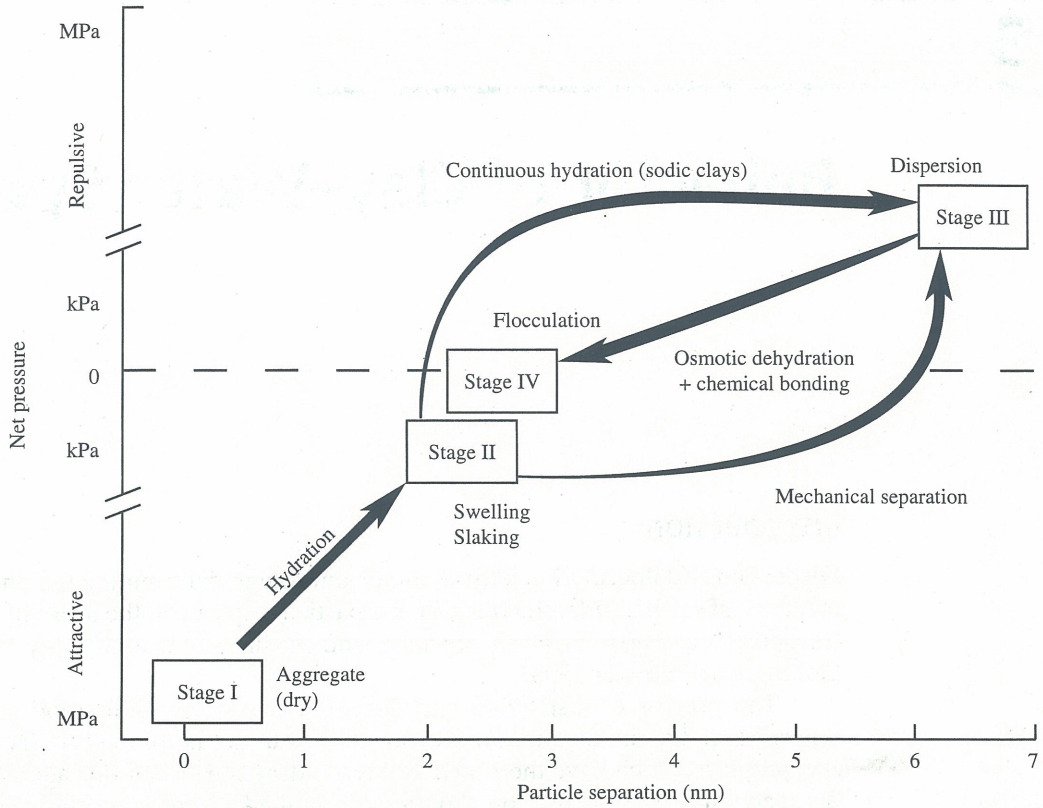

Figure 3.1 Stages of flocculation. (*Source:* Rengasamy and Sumner (forthcoming), reproduced by permission)

occurred. (For sodic clays, however, a continuous hydration occurs between stage II and stage III.) Once the system has been dispersed, flocculation (stage IV) can occur due to osmotic dehydration and chemical bonding. Progression from one stage to the next depends on the amount of water in the system (see figure 3.1).

The formation of aggregates is a result of physical, chemical, and biological processes occurring in soils (Lyklema 1978; Marshall 1964). Crusting and cracking of soils result primarily from flocculation and dispersion processes. A full understanding of aggregate formation, crusting, and cracking requires an understanding of the primary causes of separation, chemical bonding, hydration, swelling, slaking, flocculation, and dispersion of clay–water interactions (McBride 1989; Sposito 1984, 1989). These phenomena are discussed in detail in this chapter.

3.1 ELECTROCHEMICAL PROPERTIES OF CLAY–WATER SYSTEMS

Units

To avoid confusion, we will briefly digress, with a description of the units and unit systems that will be used in the following equations. Coulomb's law, as given in equation 3.1, is a fundamental law of nature and is not readily expressed in the SI unit system without adjusting the permittivity constant, ε_0. Permittivity is the ability of a dielectric to store electrical

potential energy under the influence of an electric field, measured by the ratio of the capacitance of a condenser with the material as dielectric to its capacitance (i.e., with vacuum as dielectric). Many physical chemists prefer the cgs unit system to the SI unit system for the description of electrochemical phenomena. Since the aspects of clay–water interactions greatly depend on electrochemistry, the authors share this preference. The permittivity (of a vacuum), $\varepsilon_0 = 8.854 \times 10^{-12}$ C^2 N^{-1} m^{-2}, is of great use in converting dynes to Newtons, centimeters to meters, and electrostatic units (esu) to coulombs (C).

Many of the following equations are expressed in units of one or the other system (i.e., cgs/esu or SI); but not all are written in SI units. We hope by this to encourage equal familiarity with both unit systems. As an additional help, the term $e\psi/kT$, which represents the ratio of electrical to thermal energy, is the same in both unit systems, a dimensionless number; kT is the Boltzmann constant multiplied by the absolute temperature. For example, in the cgs/esu system, e has units of esu/ion. If ψ is in esu, the product of $e\psi$ yields energy in ergs/ion with a corresponding Boltzmann constant, $k = 1.3805 \times 10^{-16}$ ergs/ion-K. One erg/esu of potential is 300 V. A useful number to remember is that $kT/e = 25.69$ mV at 25 °C. For the SI system, e is in coulombs, 1.6021×10^{-19} C/ion. In the SI system, the product of $e\psi$ yields energy in joules (J), assuming that ψ is expressed in volts (J/C). The Boltzmann constant in SI units is 1.3805×10^{-23} J/ion-K and the value for kT/e is the same, 25.69 mV at 25 °C. For conversion purposes, two useful numbers to remember are Avogadro's number (6.023×10^{23} ions/mole, etc.) and electronic charge, e (4.803×10^{-10} esu/ion).

The dielectric constant, D, is the ratio of the permittivity of the medium, ε, to that of a vacuum, ε_0, and is dimensionless: $D = \varepsilon/\varepsilon_0$. However, ε has units of esu^2/dyne · cm^2 or esu^2/erg · cm in the cgs system, and of $C^2/N \cdot m^2$ or $C^2/J \cdot m$ in the mks system. As a result, the cgs system has the advantage that permittivity is a simple number, but the disadvantage that the electric potential unit of erg/esu is not in common use.

Coulomb's Law

Coulomb's law expresses the attractive or repulsive force exerted on each other by two charged particles (say, q_1 and q_2) in a dielectric medium. If that medium is a vacuum, the law may be expressed as

$$F = \frac{kq_1q_2}{x^2} \tag{3.1}$$

where k is the dimensional proportionality constant. Physical chemists have defined the unit of electrostatic charge (esu), such that $k = 1$ dyne cm^2 esu^{-2}. The k term thus becomes numerically unimportant in equation 3.1 if cgs units are used, although it remains dimensionally necessary. In SI units, the unit of charge in common usage is C, the coulomb, which was developed from the theory of electromagnetics, rather than from electrostatics. For practical purposes, the coulomb has been determined experimentally to equal 3×10^9 esu, so that in SI units, $k = 9 \times 10^9$ Nm^2 C^{-2}.

From the theory of capacitors, the dielectric property of a vacuum has been defined as its permittivity, $\varepsilon_0 = 1/4\pi k$. Thus, in SI units, $\varepsilon_0 = 8.85 \times 10^{-12}$ C^2 Nm^{-2}. All dielectric materials have a larger permittivity than a vacuum. This property is generally characterized for a given medium by the dimensionless dielectric constant, $D = \varepsilon/\varepsilon_0$. Thus, Coulomb's law for the force exerted by charged particles in any dielectric medium can be expressed as

$$F = \frac{kq_1q_2}{Dx^2} \tag{3.2}$$

or

$$F = \frac{kq_1q_2}{4\pi\varepsilon x^2} \tag{3.3}$$

or

$$F = \frac{q_1q_2}{4\pi D\varepsilon_0 x^2} \tag{3.4}$$

Equation 3.2 is commonly written for cgs units as

$$F = \frac{kq_1q_2}{Dx^2} \tag{3.5}$$

where k, with a value of 1 dyne cm^2 esu^{-2}, is implied. To convert equations in cgs/esu to equations in SI, replace ψ by $(4\pi\varepsilon_0)^{1/2}\psi$ and q by $q/(4\pi\varepsilon_0)^{1/2}$.

In terms of the Poisson equation $\nabla^2\psi = -4\pi\rho k/\mathrm{D}$, which relates the divergence of the gradient of the potential of a specific point to the charge density of that point, we can write

$$\nabla^2\psi = -\frac{\rho}{\varepsilon_0 D} \tag{3.6}$$

where ∇^2 is the Laplace operator $(\partial^2/\partial^2x^2 + \partial^2/\partial^2y^2 + \partial^2/\partial^2z^2)$, D is the dielectric constant, ψ is the potential (volts), and ρ is esu/erg or charge per cubic meter.

Heat of Wetting

Heat is evolved when a dry soil is submerged in water or water is added to it, because water molecules lose kinetic energy in changing from a bulk form to a water film (hydration shell) on soil particle surfaces, and around cations or uncharged surfaces (Stumm 1992). This loss of energy is induced by the electric field surrounding the solid surface, which reduces the internal energy of the water molecules within this field. The water molecules are adsorbed until an equilibrium is established between the water–cation or water–clay particle. Heat of wetting increases as particle size decreases, and represents a measurement of the surface activity of the clay. Measurement of heat of wetting is used as a method to determine specific surface area (Aomine and Egashira 1970). A dry clay also exhibits a heat of wetting with solvents other than water. Likewise, heat applied to a hygroscopic body drives moisture from the body. Heat released at constant temperature is equivalent to the work done to separate the water molecules from the surface. The moisture content at which soils no longer exhibit heat of wetting is defined as hygroscopicity.

There are two types of heat of wetting: integral, and differential. Heat continues to be released as several layers of water molecules are sorbed to soil particles and their associated cations, but the outer layers are less tightly bound, and release progressively less heat. Hence, as water is added incrementally to a soil, the amount of heat produced per unit mass of added water (defined as the differential heat of wetting, i.e., the ratio of the increment of heat evolved, ∂q, to increment of water added, ∂w) decreases. The total heat produced as the medium is wetted from dryness to hygroscopy is termed the integral heat of wetting.

Several concepts can be of assistance in anticipating a range of heat of immersion values: **(1)** particles that readily wet up upon contact with water tend to have high heats of immersion and are characterized by negative values of ΔG (change in Gibbs free energy), whereas particles that do not (organic soil particles or mineral particles with organic coatings) tend to have low heats of wetting; **(2)** surfaces that possess the highest free energy have the most to gain in terms of decreasing the free energy of their respective surfaces by

adsorption; **(3)** a surface energy of about 100 mJ m^{-2} is normally the cutoff value between high- and low-energy surfaces (sand, glass, metal oxides, metal sulfides, metals and inorganic salts are good examples of high-energy surfaces); and **(4)** generally, the greater the surface area of a soil, the greater the heat of wetting can be. Solid organic compounds tend to have low-energy surfaces. In general, the harder the compound (solids), the higher the surface energy.

The heat of wetting is due to the total energy released by the adsorption of water to the surface, and is proportional to the force with which water molecules are attracted to the surface. This heat of wetting of particles may be mathematically described by

$$-\Delta H_{im} = \gamma_{LV} \cos\theta - T \cos\theta \frac{d\gamma_{LV}}{dT} - T\gamma_{LV} \frac{d\cos\theta}{dT} \tag{3.7}$$

(Adamson 1990) where γ_{LV} is the surface tension of the liquid (ergs cm^{-2} in cgs and J m^{-2} in SI), normally discussed in terms of equilibrium of the liquid with vapor; θ is the contact angle (discussed in section 4.2); and T is temperature (K). Adamson (1990) gives a value of $d\gamma/dT$ for water at 20 °C of -0.16 J m^{-2}. The contact angle, θ, is about zero for many earth materials, indicating that the surface energy of water in contact with such materials is about 120 ergs cm^{-2} or 0.12 J m^{-2}. The surface area per gram of a relatively neutrally charged material, such as silica flour, could be multiplied by this factor to obtain a very rough estimate of its heat of immersion. Consequently, the predictive capability of equation 3.7 is approximately three to four times less than the experimental evidence of Van Olphen (1969) suggests (see table 3.1).

Interaction between Uncharged Soil Particles and Water

The potential energy of the interaction, or intermolecular potential, between an uncharged clay surface and a water molecule is difficult to calculate with current technology. However, a rough approximation can be obtained by

$$Q = \sum_{n=1}^{\infty} \left(-\frac{RT}{M}\right)\left(\frac{2.3x0.88}{n^{1.80}} \times \frac{s}{(3.286\ \text{Å})^2} \times \frac{18}{N_A}\right) \tag{3.8}$$

where Q represents the heat of wetting per unit mass of clay in the same units as s, surface area per unit mass, R is the gas constant (8.31 J K^{-1} mol^{-1}), T is temperature (K), M is molecular weight of water, and n is the number of layers of water molecules sorbed to the clay surface (i.e., mass of water divided by water adsorbed onto clay to provide one molecule

TABLE 3.1 Average Heats of Wetting of Mg-Vermiculite

P/P_0^*	Adsorbed water (mg g^{-1})	Heat of wetting J g^{-1}	
0	0	232.51	
0.004	0.96	225.30	
0.018	62.58	110.91	one-layer hydrate (64.5 mg g^{-1})
0.034	83.8	89.97	
0.356	188.6	4.635	two-layer hydrate (179 mg g^{-1})
0.808	207.25	1.647	two-layer hydrate (198 mg g^{-1})

Source: Van Olphen (1969).

*Refers to relative vapor pressure (P_0 generally refers to saturated vapor pressure).

thickness). Equation 3.8 assumes that the adsorbed area of one water molecule is 10.8 Å^2, and can be written more simply as

$$Q = \left(-kT(2.3 \times 0.88) \times \frac{s}{(3.286\ \text{Å})^2}\right)\left(\sum_{n=1}^{\infty} \frac{1}{n^{1.80}}\right) \tag{3.9}$$

where k is the Boltzmann constant. The summation represents a hyperharmonic series which, for an exponent $k > 1$, converges to

$$S = \frac{2^{k-1}}{2^{k-1} - 1} \tag{3.10}$$

where S is the summation value, and for $k = 1.80$ is 2.35. Consequently, the equation can be simplified to

$$Q = (4.42 \times 10^{-19})kTs \tag{3.11}$$

with the effective area for a molecule of water incorporated into the constant. At 25 °C, this equation results in Q = 0.18 J m^{-2}. Jurinak (1963) states that, in his experiment, w_m, the mass of water sorbed to provide one molecular thickness of coverage, is 2.56 mg/g clay. This represents 8.6 × 10^{19} molecules of water, which would cover 9.25 m^2 of surface, which is presumably the specific surface area of his clay. Thus, the integral heat of wetting at an ambient temperature of 25 °C would be 1.7 J/g clay. This value is substantially smaller than measured values of the heat of wetting for kaolinite listed by Grim (1953), which range from 5 to 10 J/g. Thus, as with equation 3.7, the value will normally be about three to six times less than experimentally measured values, and is a rough approximation. While the above equations can give an approximation for heat of wetting, the most efficient way to obtain accurate values is to measure the phenomena in the laboratory. For details on laboratory methodology, the reader is referred to Anderson (1986).

Heat is also produced by wetting of clays because of hydration of the adsorbed cations. The heat of hydration of ions in free solution can be determined by the Voet (1936) equation as

$$W = -\frac{(ze)^2}{2(r + 0.7)} N_A \left(\frac{\mathrm{D} - 1}{\varepsilon}\right) \tag{3.12}$$

where W is the hydration energy (sometimes written as $\Delta G^{\circ}_{H_2O}$), z is the valence of the ion, e is 4.8 × 10^{-10} esu, N_A = 6.023 × 10^{23} (Avogadro's number), D is the dielectric constant of water, which varies with temperature (78.8 at 25 °C), r is the hydrated radius of the ion (Å), and ε = permittivity. This equation is valid when the only electric field present is that induced by the cation, and when sorbed water completely surrounds the ions in solution. Generally, heats of hydration of ions in free solution increase with ion valence, and are 86, 106, 399, 477, and 1141 kcal mol^{-1} for K^+, Na^+, Ca^{2+}, Mg^{2+}, and Al^{3+}, respectively, to name a few (Friedman and Krishman 1973).

Cations associated with clay platelets, particularly those in the Stern layer (see section 3.2), are partly bound to the clay particle, and are only partly hydrated. Hence, that portion of the heat of wetting due to ion hydration is less than that for ions in free solution. Janert, according to Grim (1953), determined efficiency ratios for various sorbed cations to be about 1/5 to 1/12, depending on ion species. Thus, the Voet equation will provide greatly erroneous (high) values for heat of immersion of clays. For example, Grim (1953) shows that kaolinite with a CEC of about 4 meq/100 g has a measured heat of immersion of 6 J/g. Assuming that the exchangeable ion is sodium, the Voet equation indicates that the heat of hydration in free

solution is about 18 J/g. Using Janert's estimate that the heat should be divided by 4.9 yields a heat of about 4 J/g. The heat of wetting varies with the nature of adsorbed cations, being higher for divalent than for monovalent, as $Ca^{2+} > H^+ > Na^+ > K^+$.

Several researchers have measured heats of wetting for various clays (Aomine and Egashira 1970). The heat of adsorption of water over varied ranges of coverage with adsorbed water for a Mg-vermiculite clay is given in table 3.2. Generally, as the initial water content increases, both the integral heat of immersion and average heat of adsorption rapidly decrease. Figure 3.2 shows the relation between heat of immersion and water content for different clays; figure 3.3 shows the heat of immersion versus surface area for various calcium-saturated clays.

TABLE 3.2 Heats of Adsorption (Average) for Mg-Vermiculite per Mole of Water in Various Ranges of Water Coverage†

	Heat of adsorption		
Coverage, n (mg g^{-1})	J mol^{-1}	kcal mol^{-1}	J g^{-1} day^{-1}
0 and 0.96	13.53×10^4	32.31	7.5
0 and 62.58	3.50×10^4	8.36	12.2
0.96 and 62.58	3.34×10^4	7.99	
62.58 and 188.6	1.52×10^4	3.63	
62.58 and 83.8	1.78×10^4	4.25	
83.8 and 188.6	1.47×10^4	3.50	
188.6 and 207.25	0.29×10^4	0.69	

Source: Data from Van Olphen (1969).
†Coverage refers to the amount of water (mg) per gram of soil. As the initial water content increases, the heat of adsorption decreases rapidly.

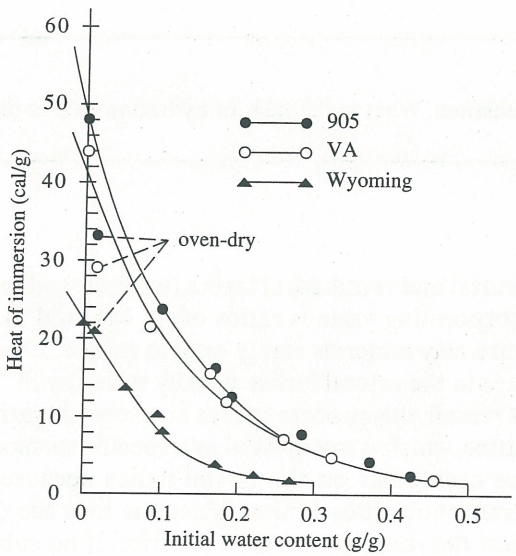

Figure 3.2 Relation between heat of immersion and water content; data from Aomine and Egashira (1970)

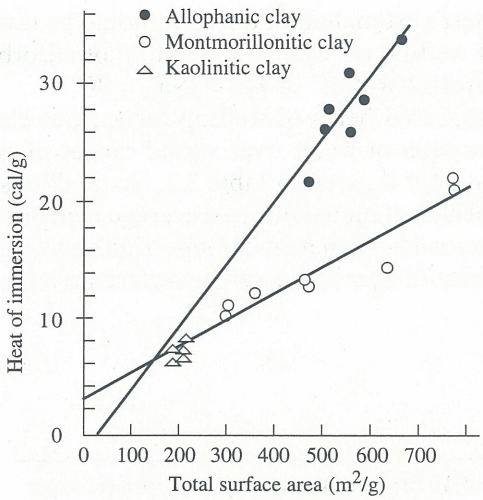

Figure 3.3 Relation between heat of immersion and total surface area for calcium saturated clays; data from Aomine and Egashira (1970)

3.2 ELECTROCHEMICAL PHENOMENA OF CLAYS

In chapter 2, we discussed how soil aggregates can be broken down into individual particles by various processes. As the aggregate is wetted, internal forces are produced. Some aggregates remain stable upon wetting, while others exhibit varying degrees of swelling, slaking, or complete dispersion. Once an aggregate has been broken down into individual particles, ionic charges associated with each particle begin to interact with neighboring particles. The charge on the particle or colloid surface tends to attract ions of opposite charge, or counterions (Grove, Fowler, and Sumner 1982; Verwey and Overbeek, 1948). Such ions tend to diffuse through the soil water in an attempt to equilibrate concentration. As a result, the colloid becomes surrounded by a diffuse cloud of ions, which has come to be known as the diffuse electrical double layer. Various theories that have been proposed to predict the behavior of colloids as affected by the double layer, including van der Waals forces, will be presented in this and subsequent sections.

QUESTION 3.1

An electrical field is induced by potassium. What is the heat of hydration of this ion? (Assume a dielectric constant of 80.)

Surface Charge of Clay Minerals

As clay minerals form, the octahedral and tetrahedral layers (as discussed in chapter 2) bind together one layer at a time, incorporating various ratios of Al, Mg, and Si. Because of the variable ratio of these cations, pure clay minerals rarely exist in nature. During mineral formation, Al^{3+} ions may occupy sites in the crystal lattice usually taken by Si^{4+} ions, and Mg^{2+} or Ca^{2+} may displace Al^{3+} ions. Overall, this process causes an excess negative charge of the clay particle within the crystal lattice, which is manifested as a specific surface charge density. These particular ions can replace each other on the crystal lattice because of their similar size; the process is known as isomorphous substitution. Since the ions are of like size, their substitution does not usually affect the shape of the crystal lattice. If no substitution occurs, the clay particle will remain electrically neutral.

Diffuse Electrical Double Layer Theory

Clay particles are electronegatively charged for three reasons: **(1)** There is an isomorphous substitution of Al (trivalent) for Si (tetravalent) that leaves an excess negative charge

$$O^{--}Si^{++++}O^{--} \rightarrow O^{--}Al^{+++}O^{--}$$

(2) There are broken bonds on crystal edges or ionization of hydroxyl groups attached to silicon of broken tetrahedral planes (i.e., silicic acid),

$$Si\text{-}OH + H_2O \rightarrow SiO^- + H_3O^+$$

and, **(3)** The presence of silicic or phosphoric acid can form an integral, clay particle surface giving rise to a negative charge as well.

The electronegative charge of clay particles implies that a clay–water system is capable of doing work on the anion; thus, potential energy will vary between points within the bulk solution (Sposito 1984). The potential at a point near a clay particle is defined as the work that must be done to induce a unit negative charge from the bulk solution up to that point. Because clay is negatively charged, the unit negative charge is used rather than the conventional positive charge of electrostatic potential.

This overall negative charge is compensated by exchangeable cations held to the clay surface by coulomb forces. The combination of a negative charge on the clay surface and a counteracting charge from the cations creates an electrical double layer around individual clay particles. The effect of this double layer is to make the clay–water system electrically neutral. An anion placed near a clay surface is pushed away by electrostatic repulsion forces between the clay particle and the anion.

Several scientists have derived mathematical expressions for potential as a function of distance from a clay particle, among them Helmholtz (1879), Gouy (1910), Chapman (1913), Debye and Huckel (1923), and Stern (1924). The most commonly discussed expressions or models include the Helmholtz parallel-plate capacitor, the Gouy–Chapman diffuse double layer, and Stern's double layer theory.

Helmholtz suggested that the electrical double layer had a fixed thickness of one molecule that was generally formed at the particle/solution interface. He believed that the inner, negatively charged layer was rigid, adhering firmly to the solid surface, whereas the outer layer of oppositely charged (+) ions in the solution was mobile. Helmholtz's theory represents the clay platelet as a simple parallel-plate capacitor. Because of thermal motion, counterions are distributed within a certain space forming a diffuse layer; consequently, this does not permit a rigid formation at the interface as Helmholtz suggested.

Guoy–Chapman proposed a diffuse double layer in which the negative charges are adsorbed primarily near the solid surfaces and the positively charged ions are distributed away from the surface. The cation concentration near the surface is dense and decreases exponentially with distance, until the net charge density is zero. This exponential distribution occurs because the high cation concentration near the particle is partially counteracted by a tendency for diffusion away from the colloid surface. Local cation concentration is calculated by the Boltzmann equation:

$$n^+ = n_0 \exp \frac{-ze\psi}{kT} \tag{3.13}$$

where n^+ is ion concentration at a specified distance from the charged surface, in ions cm^{-3} (figure 3.4); n_0 is ion concentration in bulk solution (ions cm^{-3}); z is ion valence (dimensionless); e is the unit of electronic charge (coulomb/ion in the SI system, or esu/ion in the cgs/esu system); ψ is the electrical potential of the colloid at the specified distance (ergs/esu or volts);

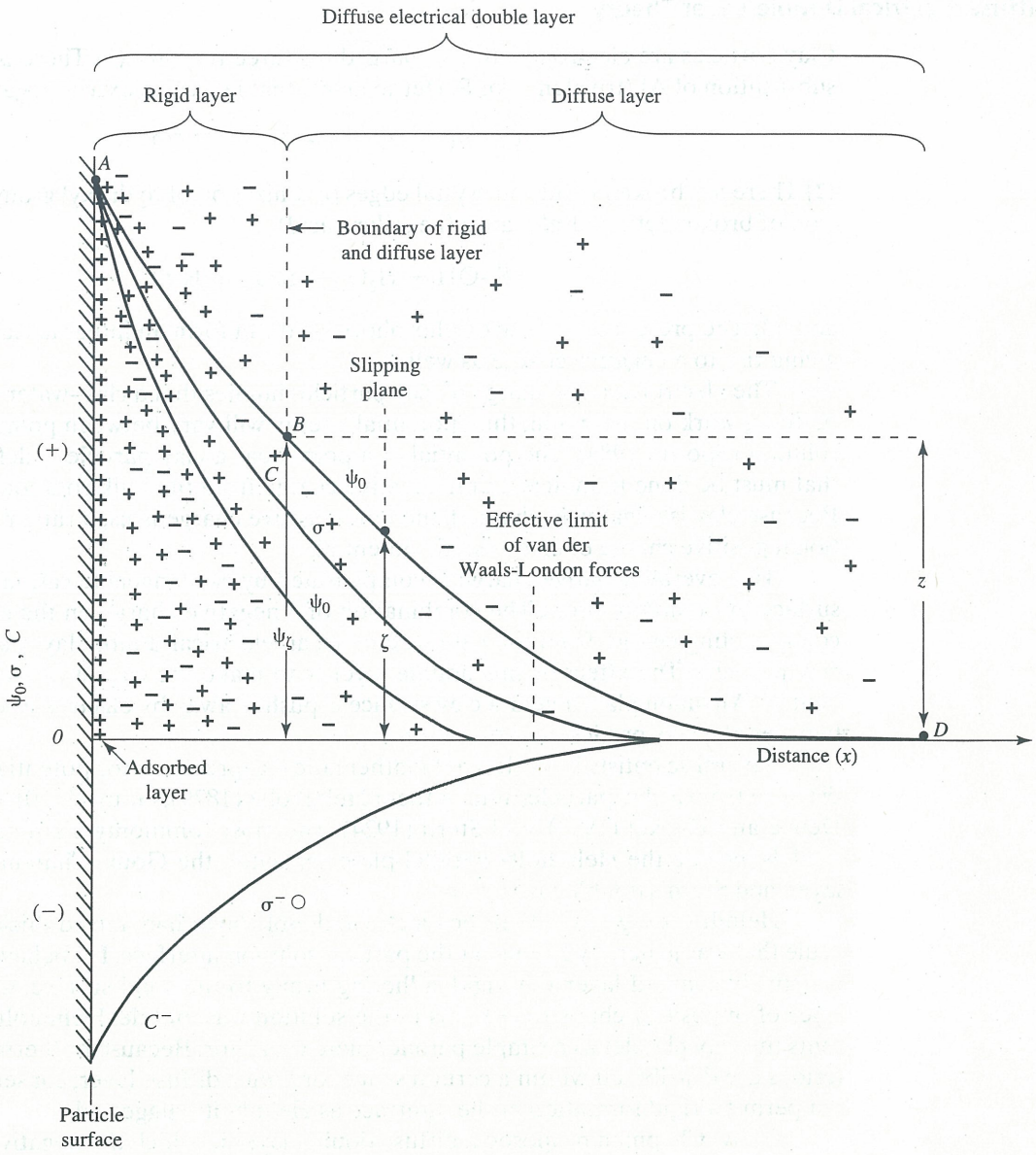

Figure 3.4 Representation of the diffuse electrical double layer

k is the Boltzmann constant (gas constant per molecule, J; or ergs per molecule, K or J K^{-1}); and T is absolute temperature, K.

Anions are repelled by the negative charge of the particle, resulting in a sparse distribution near the particle that increases exponentially with distance, also given by Boltzman's equation:

$$n^- = n_0^- \exp \frac{+ze\psi}{kT} \tag{3.14}$$

These equations for cation and anion distribution may be combined to develop a relation between the character and concentration of an equilibrium solution and the electrical

charge induced by the surface of a colloid. This relation is expressed as

$$\sigma = \left(\frac{2\varepsilon nkT}{\pi}\right)^{1/2} \sinh\left(\frac{ze\psi_0}{2kT}\right) \tag{3.15}$$

where σ is the charge on the colloid surface (esu cm^{-2} or, if k is replaced by R, meq cm^{-2}); ε is the permittivity of water (esu^2 dyne^{-1} cm^{-2}); n is the electrolyte concentration in solution (ions cm^{-3}—this unit is achieved by converting with Avogadro's number); k is the Boltzmann constant; T is absolute temperature; z is the valence of counterions; e is the electric charge (esu/ion); and ψ_0 is the electric potential (ergs/esu) at the colloid surface.

The diffuse double layer into the surrounding equilibrium solution can be thought of as having an effective thickness (κ^{-1}). Theoretically, due to the exponential nature of the relation between ion concentration and distance, the double layer is infinite in thickness. However, if we assume that a cloud of ions, concentrated as a point, planar charge, is at a distance from the colloid surface similar to that of an electrical condenser (the Helmholtz theory), double layer thickness then can be expressed as

$$\kappa^{-1} = \left(\frac{\varepsilon kT}{8\pi z^2 e^2 n}\right)^{1/2} \tag{3.16}$$

where all units are as defined for equation 3.15. This effective thickness is analogous to the atmospheric scale height; and for small values of surface potential, the Guoy distribution of potential with distance x from the surface is given by $\psi x = \psi_0 e^{-\kappa x}$. This relation is shown in figure 3.4. Van Olphen (1963) used the preceding equation to compute κ values for solutions of 10^{-1}, 10^{-3}, and 10^{-5}, M concentration with $1/\kappa$ ranging from 10^{-5} to 10^{-7} cm for single valent ions.

Stern showed that neither the sharp, rigid Helmholtz theory, nor the Guoy-Chapman diffuse double layer theory were adequate, and proposed a theory that combined features of the two. Stern proposed a negative charge rigidly attached to the surface of the clay particle, with an adjacent layer of positively charged cations (Stern believed this layer to be about the diameter of one cation in thickness with a sharp drop in potential, as in the Helmholtz theory). As distance increases towards the bulk solution, the remaining part of the double layer becomes diffuse in character (as in the Gouy-Chapman theory). In the rigid portion of the double layer, the ions are mostly immobile, whereas in the diffuse layer, thermal agitation permits the ions to move freely. Within the rigid layer, cations are preferentially adsorbed, which results in a gradual decrease in potential in the bulk solution that contains a uniform charge distribution (figure 3.4). The actual thickness of the diffuse layer is undefined since it depends on both the type and concentration of the ion present. However, common thickness is measured in angstroms, and can vary from < 10 Å to > 400 Å.

The interface between the fixed and diffuse layers is not sharp, and should be thought of as a boundary where some ions are migrating to the clay particle and others are shearing away. This becomes clear if it is assumed that a clay particle has its own ionic atmosphere, and is within an electrical field. Readers should note that, in the following discussion, we use the Gouy-Chapman theory, due to the difficulty of applying the Stern theory (which can lead to ludicrously high local counterion concentrations, because the ions are considered as point charges and are presumed present at the colloid wall where electric potential is highest).

QUESTION 3.2

What is the cation concentration in a solution 12 Å from a clay surface? Assume a monovalent ion, $C_0 = 2.5 \times 10^{-2}$ M, $T = 25$ °C, $\psi = 100$ mV, and $e = 4.803 \times 10^{-10}$ esu ion^{-1}.

QUESTION 3.3

What is the electrical charge induced by the surface of a clay platelet in a solution of 3.1×10^{-2} M NaCl solution at 25 °C? Assume $\varepsilon = 78.8$ esu^2/erg cm and $\psi_0 = 75$ mV.

3.3 ELECTROKINETIC PHENOMENA

Electrophoresis

The term electrophoresis refers to the movement of charged particles in relation to a stationary solution, that is, in an electric field. Envision a clay particle and associated charge placed into an electric field; since the clay particle is negatively charged, it will tend to migrate in the positive field direction. Ions near the clay particle surface migrate with the particle, whereas those further away in the solution will slip away from the particle surface and migrate in the opposite direction of the electric field.

The slipping plane indicated in figure 3.4 divides ions in the double layer into those migrating with the clay particle and those shearing away from it. The potential drop between the slipping plane and bulk solution is the zeta potential, which is the work per unit charge required to move an anion from the bulk solution to the slipping plane (Sennett and Olivier 1965). The zeta potential is represented by the voltage difference between point D and point B in figure 3.4. The zeta potential is affected by cation density in solution: if cation density is decreased, charge density is also decreased, which results in a larger thickness of the cation layer, resulting in a thicker double layer. Likewise, if the cation concentration present in solution increases, a thinner double layer will result. The thicker the double layer becomes (assuming charge density remains constant), the higher the zeta potential will be. This is because the further the cations extend from the particle surface into the diffuse layer, the greater will be the number of cations to the right of the slipping plane (figure 3.4). This hypothesis assumes that the number of cations increases faster in the bulk solution with distance from the particle than the electric field of the capacitor, and that the zeta potential is not too large. The zeta potential is given by

$$\zeta = \frac{4\pi\sigma d}{\varepsilon} \tag{3.17}$$

where ζ = zeta potential (volts), σ = surface charge density (esu cm^{-2}), d = distance (cm), and ε = permittivity of the solution (esu^2 erg^{-1} cm^{-1}) Equation 3.17 is greatly simplified, and indicates a linear increase in potential from the charged surface when it should reflect an exponential decrease. Mitchell (1993) expresses the zeta potential as $\zeta = \sigma\delta/\mathrm{D}$, where δ is the distance between the wall and the center of the plane of mobile charge, and D is the relative permittivity or dielectric constant of the pore fluid. To rigorously derive this equation one must begin with Poisson's equation and the Boltzmann distribution. Additional theory and applications of zeta potential may be found in Sennett and Olivier (1965), and Babcock (1963).

The velocity of particle movement during electrophoresis is that at which coulombic force, $\zeta\varepsilon E_s$, is balanced by viscous force, $4\pi\eta v$, as described by Stoke's law (see section 2.5). Thus,

$$V = \frac{\zeta\varepsilon E_s}{4\pi\eta} \tag{3.18}$$

where V is electroosmotic velocity, E_s is potential gradient, ε is the permittivity of the solution, the numeral 4 is for cylindrical shapes (this would be replaced by 6 for spherical shapes),

and η is the fluid viscosity, Pa s. The Dorn effect is the reverse of electrophoresis, and is the potential difference resulting when particles fall through a solution due to gravity.

QUESTION 3.4

Assuming a parallel-plate capacitor, calculate the zeta potential 23 Å from particle surface. Assume $\varepsilon = 78.8$, $e = 4.8 \times 10^{-10}$ esu ion^{-1}, and that the media is montmorillonite with a CEC of 1.5×10^{-7} meq cm^{-2} and a surface area of 650 m^2/g.

Electroosmosis

During the process of electroosmosis, water movement occurs when a moist soil is placed between two electrodes and subjected to an external electrical potential difference; cations in the double layer migrate (by electrostatic attraction) towards the cathode, or negative pole, while the anions migrate toward the anode, or positive pole (Adamson 1990; Ghildyal and Tripathi 1987; Stumm 1992). (See figure 3.5.) The cations translocate in the electric field and, while doing so, pull with them the oriented water molecules. This water layer is now positively charged and becomes mobile, dragging the remaining water along the immobile part of the liquid film. The rate of flow depends on the magnitude of the electrical potential difference and the viscosity of the liquid; as with electrophoresis, the velocity of water movement is determined as that at which viscous drag equals the coulombic force exerted by the electric field. Microscopically, the electric force in the capillary is applied to the ions within the fluid and not directly to the water.

During electroosmosis, the electrolyte in the capillary is acted on by electric and viscous forces; there are other forces, however, including mechanical, pressure, inertial, and surface tension, that produce effects that act on the electrolyte, and that are often inseparable from those of electroosmosis. The movement of water in the capillary is determined by the effects of all forces, with the primary forces being electrical, thermal, and viscous. Esrig and

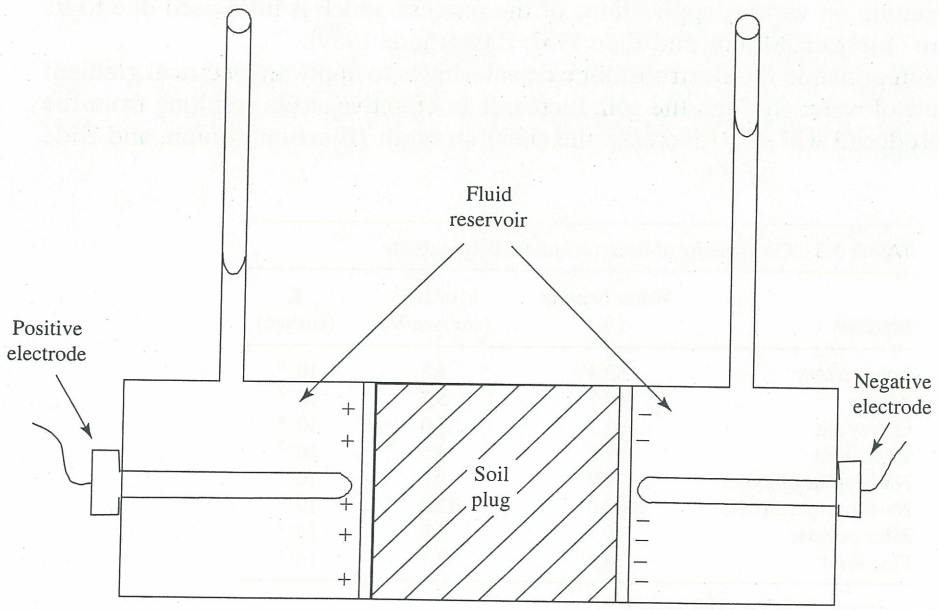

Figure 3.5 Apparatus for measuring electroosmotic pressure; data from Adamson (1990)

Majtenyi (1965) describe the total electric field as the negative gradient of the sum of existing potentials. For electroosmosis, electrical potentials are of three types: potentials applied by electrodes, potentials created by ions other than the one being considered, and potentials created by dipoles. For example, the electrical force on a dipole (water molecule) depends on the dipole moment and gradient of the electric field.

Thermal phenomena can influence electroosmotic water flow by causing either geometrical or physical changes in the capillary system. Such changes generally correspond to variations in temperature. If a concentration gradient exists, thermal agitation of molecules and particles within the capillary system will produce a tendency towards equilibrium. Changes in physical conditions may not be accompanied by changes in geometry if the temperature of the capillary system remains constant. Geometric changes occur due to volume expansions or contractions of the capillary fluid, or of the solid portion of the medium when subjected to a temperature fluctuation.

Viscous forces depend on the velocity gradient, dv/dn, and the coefficient of viscosity, μ. The viscous force, V_f, for a volume element, dv, on a surface element, dS, is given as

$$dV_f = \mu \frac{\partial^2 V}{\partial n^2} dv \tag{3.19}$$

where n is normal to the surface and V is velocity.

Electroosmotic hydraulic conductivity, k_e, indicates flow velocity under a unit electrical gradient. Three common theories are used to predict k_e: the Helmholtz and Smoluchowski theory (pore water flow occurs in a large soil pore); the Schmid theory (pore water flow occurs in a small soil pore); and the Spiegler friction model (flow is considered as a result of interactions of mobile water molecules and ions). These theories are discussed in detail in Mitchell (1993). In contrast to soil water hydraulic conductivity, which varies with the square of effective pore size, k_e is relatively independent of pore size. Mitchell (1993) shows a general range of 1×10^{-9} to 1×10^{-8} m^2/s/volt (m/s per volt/m); and that regardless of soil type, k_e is on the same order of magnitude. However, hydraulic conductivity changes by several orders of magnitude for the same material (see table 3.3). A knowledge of k_e can sometimes provide an efficient means of dewatering soils, which has proven useful for temporary stabilization during excavation. This technique was first used in the 1930s by Casagrande, who compiled information on various applications of the process, which is little used due to its expensive nature (Bjerrum, Moum, and Eide 1967; Casagrande 1959).

The common principle for electroosmotic dewatering is to apply an electrical gradient to produce a flow of water through the soil. Increases in effective stress resulting from the flow of water produced will often increase the shear strength (Bjerrum, Moum, and Eide

TABLE 3.3 Coefficients of Electroosmotic Permeability

Material	Water content (%)	k_e in 10^{-5} (cm^2/sec-V)	K (cm/sec)
London clay	52.3	5.8	10^{-8}
Kaolin	67.7	5.7	10^{-7}
Clayey silt	31.7	5.0	10^{-6}
Rock flour	27.2	4.5	10^{-7}
Na-Montmorillonite	170.0	2.0	10^{-9}
Na-Montmorillonite	2000.0	12.0	10^{-8}
Mica powder	49.7	6.9	10^{-5}
Fine sand	26.0	4.1	10^{-4}

Source: Data from Mitchell (1993).

1967). This process typically has been used for silt or silty soils of medium permeability, but Bjerrum, Moum, and Eide (1967) showed that it could be used for soft clays as well. In their experiment, they increased soil strength, due to consolidation, from an initial value of less than 1 t/m^2 to an average value of 4 t/m^2. In electroosmosis, dewatering occurs when water is drawn to a cathode, where it is drained away, and no water is allowed to enter at or near the anode. This results in a consolidation and, therefore, stabilization of the soil between the electrodes, which is equal to the volume of water removed.

In chapter 2, we discussed soil profiles, composition, and geometry. In a typical soil, some particles are in contact due to consolidation pressure. Such particles can be considered to be the "skeleton" of a soil. Other particles may be surrounded by water. If we apply an electric field to this system, a migration of charged particles might result; that is, electrophoresis. The occurrence of electrophoresis indicates that soil particles are migrating against the flow of water. This is especially true in clays. Such particles can be obstructed by the soil skeleton, resulting in clogged capillaries and a restriction of water flow. This is an undesirable condition when electroosmotic dewatering is attempted in soils. In this regard, particle size distribution is very important and should be examined carefully, particularly the colloidal fraction as it exhibits the greatest electrochemical activity. These conditions can geometrically alter the capillary system.

Changes in matric potential or soil pressure can alter the geometry of the capillary system (Sposito 1989). For example, when a dry clay comes in contact with water, an increase in pressure results, which may cause the displacement of soil particles and alteration of pore geometry. This will create a new condition for electroosmotic flow. All soil characteristics must be known before attempting to calculate electroosmotic flow. Various laboratory tests will provide information on soil porosity, mineralogy, surface area, water content, degree of saturation, pore size distribution, charge density, hydraulic conductivity, particle size analysis, and other chemical and physical parameters, including capillary orientation with respect to the direction of the applied electric field.

Esrig and Majtenyi (1965) have given the total outflow per unit time (assuming cylindrical capillary), Q, from a soil mass as

$$Q = C_r \frac{\pi}{2\mu} \left(\sum_n m_n \overline{\rho_n} \left(R_n^3 \cdot d_n - 0.75 \cdot R_n^2 \cdot d_n^2 \right) \right) \cdot A \cdot E \tag{3.20}$$

where C_r is a coefficient to account for assumptions in double layer thickness and effective capillary radius, which will vary between 0 and 1 and will be less than unity for all soils; m_n is the number of capillaries of radius R_n per unit cross-sectional area A; d is double layer thickness; ρ_n is the average mobile charge density ($q\ L^{-3}$); and E is electric field strength ($M\ L\ T^{-2}\ q^{-1}$). By analogy to Darcy's law, $Q = k_e AE$, where k_e, the electroosmotic permeability of a soil, is expressed as

$$k_e = C_r \frac{\pi}{2\mu} \left(\sum_n m_n \overline{\rho_n} \left(R_n^3 \cdot d_n - 0.75 \cdot R_n^2 \cdot d_n^2 \right) \right) \tag{3.21}$$

This equation can take several different forms, depending on soil physical characteristics. The velocity of electroosmotic flow is independent of capillary radius and cross-sectional area, if the capillary is large enough to ensure that the double layer along each wall does not interact. For large capillaries, the volume outflow per unit time can be related to porosity (Esrig and Majtenyi 1965). If capillary radius is small and double layers interact, electroosmotic flow velocity will depend on the curvature of the capillary wall and upon capillary radius; the volume of outflow per unit time for such capillaries cannot be related to soil porosity. For a more detailed discussion of electroosmosis, the reader is referred to Adamson (1990), Mitchell (1993), and Esrig and Majtenyi (1965).

Streaming Potential

Unlike electroosmosis, in which a liquid flows along a charged surface when an electric field is applied parallel to the surface (in the liquid), the streaming potential is a measure of the electric potential created when a liquid is forced to flow along a charged surface. As water in a soil moves near a fixed clay surface, some of the cations in the diffuse layer will be carried with it. However, these cations resist the movement due to their attraction to the negatively charged surface of the clay particles. This resistance creates a drag force (F_d) on the water, causing it to move less rapidly. As explained in the description of electrophoresis, F_d is affected by cation density in solution.

Consider a column of soil: as water percolates through the column, the cation concentration at the outflow end of the column will be greater than at the inflow end. Consequently, as water continues to move through the column, increased pressure will be needed at the inflow end to maintain the same rate of flow, because the water must move cations in the solution against the repulsive force of the increased number of cations (increased charge density) at the outflow end. Generally, this will create a measurable potential difference across ends of the column, known as the streaming potential. The streaming potential is the reverse of electroosmosis. Because streaming potential can be measured directly during a measurement of hydraulic conductivity (using a high impedance voltmeter and reversible electrodes), one can obtain an estimate of electroosmosis using Saxen's law (Mitchell 1993).

The streaming potential may be expressed as

$$E_s = \frac{\zeta P \varepsilon}{4\eta\pi\lambda'} \tag{3.22}$$

where E_s is the induced streaming potential (volts), P is the net pressure necessary to stop the water flow (Pa), η is fluid viscosity (Pa s), and λ' is the specific or electrical conductivity of water (ohms or μohms cm^{-1} in the cgs system and dS m^{-1} in the SI system).

According to Saxen's law, the prediction of electroosmosis from streaming potential is given by

$$\left(\frac{q_h}{I}\right)_{\Delta P=0} = -\left(\frac{\Delta E}{\Delta P}\right)_{I=0} \tag{3.23}$$

where q_h is the hydraulic flow rate, I is the electric current, ΔP is the pressure drop, and ΔE is the electrical potential drop. Equation 3.23 was first shown experimentally by Saxen (1892), and has been verified for clay–water systems.

QUESTION 3.5

What is the double layer thickness at the surface of a clay platelet suspended in a solution of 10^{-2} M NaCl? Assume $T = 25$ °C and $\varepsilon = 78.8$. Use Avogadro's number for conversion units.

QUESTION 3.6

What is the linear electroosmotic velocity of flow for a liquid plug in a column 1 m long? Assume $\zeta =$ 60 mV and an applied voltage drop of 100 V across the column.

3.4 THE DLVO THEORY OF COLLOID STABILITY

The DLVO theory was proposed independently by Derjaguin and Landau (1941) and Verwey and Overbeek (1948); hence, the theory goes by their combined initials. Derjaguin and Landau (1941) describe the repulsive force between particles, whereas Verwey and

Overbeek (1948) consider the repulsive energy. The end result is basically the same, however. Both theories assume that clay particles (colloids) are planar in shape. The DLVO theory describes the repulsion of clay particles in close proximity that have an interacting double layer and in which there is an associated interaction (both attraction and repulsion) between van der Waals–London forces associated with each particle. Because the diffuse double layer extends some distance from a particle, as particles are brought together, their respective double layers interact. Consequently, a repulsive force exists, and a potential energy has to be overcome to bring particles together. The DLVO theory predicts the energy associated with interaction as a function of interparticle distance. Given a repulsive force, as a function of the distance $2d$ between two clay platelets, the potential energy, V_R, is reversible and isothermal (Gibbs free energy), and is described by

$$V_r = 2\int_{-\infty}^{d} P\,dz \tag{3.24}$$

where V_r is the potential energy (ergs cm^{-2}), d is the particle diameter (cm), and P is the pressure exerted on the plane midway between the two particles (in ergs for the cgs system, and Pa for SI). This pressure can also be considered the external pressure (P_e) applied to the outside surface of each particle (figure 3.6).

Interactive Repulsive Forces between Platelets

From the Kelvin–LaPlace equation, the chemical potential of soil water at point X (figure 3.6) in the solution away from the particles or plates is determined by

$$\begin{aligned}\mu_X &= \mu_0 + Z_X g\rho = -\frac{RT}{M}\sum x_i + Z_X g\rho = -\frac{RT}{M}\left(\frac{2n_0}{1M^{-1}}\frac{1}{N_A}\right) + Z_X g\rho \\ &= -2kTn_0 + Z_X g\rho\end{aligned} \tag{3.25}$$

where μ_0 (n_0 in figure 3.6) is the decrement in chemical potential due to ions in solution; M is the molecular weight of water (g); x_i is the mole fraction of ith ions; $2n_0$ is the number of ions per cm^3 in the solution; k is the Boltzman constant; Z_x is the increment in distance from standard height to height of point X; g is the gravitational constant; and ρ is the density of

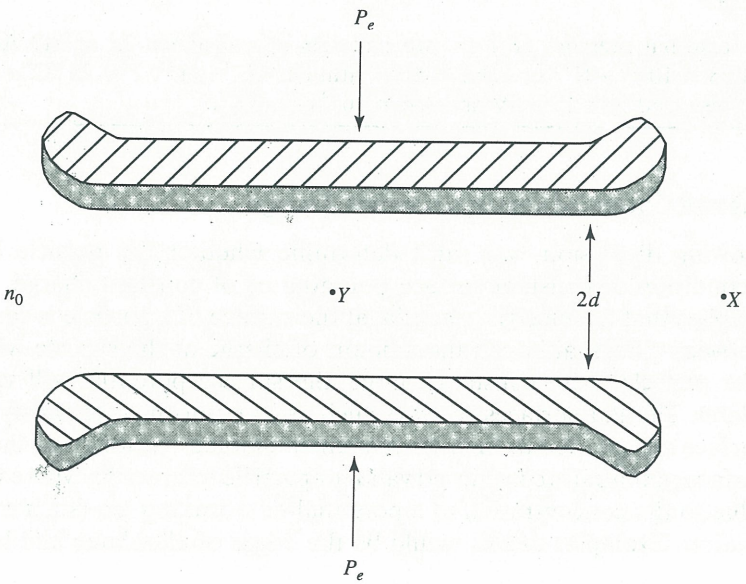

Figure 3.6 Representation of repulsive force acting between two charged clay platelets

solution. The term $2kTn_0$ will have units of dynes/cm^2 (cgs system) or Pa (SI system). The chemical potential at point Y is given as

$$\mu_Y = \mu_f + \mu_0 + \int_0^{P_i} \overline{v_w}\, dP + Z_Y g\rho \tag{3.26}$$

where P_i is the internal pressure between the particles and v_w is the partial volume of water. This equation can be simplified by assuming that $\mu_f << \mu_0$ (negligible), and $v_w = 1.0$ and is independent of pressure. Thus,

$$\mu_Y = \mu_0 + P_i + Z_Y g\rho \tag{3.27}$$

Because $P_i = P_e$, cations and anions at point Y are expressed as

$$n^+ = n_0 e^{-ze\psi_d/kT} \qquad n^- = n_0 e^{ze\psi_d/kT} \tag{3.28}$$

where n^+ represents cations, n^- represents anions, and z is ion valence. To simplify the following equations, we will let $y_d = ze\psi_d/kT$. Consequently, the potential at point Y can be expressed as

$$\mu_Y = kTn_0(e^{-y_d} + e^{y_d}) + P_e + Z_Y g\rho \tag{3.29}$$

assuming that the system is at equilibrium $\mu_X = \mu_Y$ and $Z_X = Z_Y$; so

$$-2kTn_0 = -kTn_0(e^{-y_d} + e^{y_d}) + P_e \tag{3.30}$$

To calculate the external pressure (P_e) on the two plates (assuming $P_e = P_i$), equation 3.30 can be rearranged to obtain

$$P_e = n_0 kT(e^{-y_d} + e^{y_d} - 2) = 2n_0 kT[\cosh(y_d) - 1] \tag{3.31}$$

which also assumes that the distance between the two plates is $2d$ (two times the particle thickness).

Note: The equations just developed also apply to clay swelling. Thus, the equations developed to describe the pressure field generated by coulombic forces are exactly the same whether we consider the particles as separate entities or as layers of a montmorillonite grain in which internal layers are subject to formation of the double layer.

QUESTION 3.7

What is the external pressure (P_e) on two platelets at a distance $2d$ apart? Assume $n = 0.01$ N, $z = 1$, $k = 1.38 \times 10^{-23}$ J K^{-1} or 1.363×10^{-22} atm cm^3 K^{-1} ion^{-1}, $T = 25$ °C, $e = 1.6 \times 10^{-19}$ C or 4.803×10^{-10} esu, and $\psi_d = 100$ mV or 3.366×10^{-4} erg esu^{-1}.

Potential Energy due to Constant Potential versus Constant Charge

In the following discussion, one must determine whether the particle being considered satisfies a condition of constant surface potential or of constant charge. Constant surface potential implies that the electric potential at the surface of a particle is constant despite the distance between plates, although the amount of charge at the surface will depend on this distance. For particles with constant charge, the surface potential will vary with distance between plates. The flat surfaces of clays such as montmorillonite satisfy the condition of constant surface charge, due to their permanently charged nature. Also, the assumption of a constant surface potential is considered valid for particle interaction where the surface charge density is due to the concentration of a potential-determining ion (such as H^+) in the equilibrium solution. Examples of this would be the edges of allophane and kaolinite particles.

Mathematically, the interactions between constant potential and constant charge surfaces are very different. However, for weak interactions and large distances there is little difference.

Equation 3.24 is difficult to integrate. To obtain the potential energy due to repulsive forces, V_R (erg cm^{-2}), we may substitute equation 3.31 into equation 3.24:

$$V_R = -2\int_{\infty}^{d} [2n_0kT(\cosh(y_d) - 1)]\,dz \tag{3.32}$$

Care must be taken when integrating equation 3.32, as its calculation will vary depending on constant charge or constant potential; units will be in ergs/cm^2. For the case of constant potential, the potential at the surface of the colloid remains constant irrespective of distance between particles; the repulsive energy between platelets separated by a distance, d, is

$$V_R^{\psi} = 2\frac{n_0e^2(\psi_0^{\infty})^2}{kT\kappa}e^{-2\kappa d} \tag{3.33}$$

where κ (m) is as expressed in equation 3.16, and ψ_0^{∞} represents constant surface potential at infinite particle separation. For spherical colloids at constant potential, assuming the electric potential at the particle surface is < 3 mN/m^2, the repulsive energy is given by

$$V_R^{\psi} = \frac{\varepsilon r(\psi_0)^2}{2}\ln[1 + \exp(-\kappa H)] \tag{3.34}$$

where ε is the permittivity of the solution, r is the radius of the particle, and H is the minimum separation of the two particle surfaces.

Under constant charge, potential varies with distance between particles. This condition is satisfied in soil systems of typical clays (such as kaolinite or montmorillonite) that are platelike in shape. The potential for the surface of constant charged particles depends on whether $e\psi_d/kT$ (dimensionless) is small or large. For cases where the potential is < 0.1 J/C or V, the repulsive force is expressed as

$$V_R^{\psi} = \frac{2n_0kT}{\kappa}(y_0^{\infty})^2\left(\coth\frac{\kappa d}{2} - 1\right) \tag{3.35}$$

where d is distance between plates. When the potential > 0.1 J/C or V, the repulsive force is expressed as

$$V_R^{\psi} = \frac{2n_0kT}{\kappa}\left\{2y_0^{\infty}\ln\left[\frac{B + Y_0^{\infty}\coth\left(\frac{\kappa d}{2}\right)}{1 + y_0^{\infty}}\right] - \ln[(y_0^{\infty})^2 + \cosh(\kappa d) + B\sinh(\kappa d) + \kappa d]\right\} \tag{3.36}$$

where $y_0^{\infty} = e\psi_0^{\infty}/kT$ and $B = \sqrt{1 + (y_0^{\infty})^2\operatorname{csch}^2(\kappa d/2)}$ (Verwey and Overbeek 1948; Wilemski 1982).

The repulsive force for energy between two spherical particles of equal dimension is given by

$$V_R = V_R^{\psi\infty} - \frac{\varepsilon r(\psi_0^{\infty})^2}{2}\{\ln[-\exp(-2\kappa H)]\} \tag{3.37}$$

where $V_R^{\psi_0^\infty}$ is the repulsive energy between particles of constant surface potential ψ_0^∞ (which represents the electric potential at the particle surface when the particle separation is infinite) and r is the particle radius. Thus,

$$V_R^{\psi} = \frac{\varepsilon r(\psi_0)^2}{2} \ln[1 + \exp(-\kappa H)] \tag{3.38}$$

When dealing with constant charge parameters, the left side of equations 3.32–3.37 might be more appropriately labeled with the superscript σ to denote constant charge density (i.e., V_R^σ). A general relationship of V_R versus distance is given in figure 3.7.

QUESTION 3.8

Determine the repulsive force (V_R) for a spherical colloid, assuming a small electrical potential. Also, determine this force for a platelet-shaped particle.

Van der Waals–London Forces

Van der Waals–London forces exist between neutral nonpolar molecules; they do not depend on a net electrical charge, and are independent of ionic strength of solution in most aqueous systems. Thus, they can be thought of as short-range, electrostatic attractive forces. In 1930, Fritz Wolfgang London (1900–1954) used quantum mechanics to quantitatively express this force. Neutral atoms constitute systems of oscillating dipole charges ($> 10^{15}$ Hz) resulting from the variable orbital location of negatively charged electrons about the positively charged nucleus. At distances > 100 Å, quantum mechanics predicts that an atom cannot polarize an adjacent atom. Van Olphen (1963) and others report that van der Waals–London forces are additive. Because these forces are additive, the attraction between particles which contain a large number of atoms is equal to the sum of the attractive forces for each atom pair; the total attractive force can become quite large. Force decays less rapidly with distance for large particles containing large numbers of atom pairs. Van der Waals–London forces between colloidal particles vary between the inverse of the 3rd and 7th power of the distance between the particles. These forces strongly affect the flocculation of clay particles in soil–water systems, but contribute little to the attraction between water–clay interfaces.

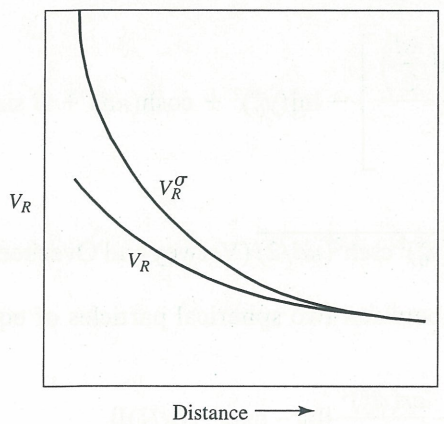

Figure 3.7 General relation of potentials; constant potential, V_R, and constant charge, V_R^σ.

Potential Energy Due to van der Waals–London Forces

As for repulsive forces, the concepts of energy due to van der Waals–London forces apply to both platelet and spherical shapes. For particles of platelet shape, the attraction energy in ergs cm^{-2} (V_A) is given as

$$V_A = -\frac{A}{48\pi}\left[\frac{1}{d^2} + \frac{1}{(d+\delta)^2} - \frac{2}{(d+\delta/2)^2}\right] \tag{3.39}$$

(van Olphen 1963), where A is the Hamaker constant $[\pi^2 n^2 (3/4) h v_o \alpha^2]$ (Adamson 1990); n is molecules per cm^3; h is the Planck constant (ergs · s); v_o is the activation or London frequency (s^{-1}); α is the polarizability (cm^3); and δ is the plate thickness at distance $2d$ (two times the plate thickness or diameter). The potential of the van der Waals forces, ψ, between two atoms is

$$\psi = -\frac{c}{r^6} \tag{3.40}$$

where r is the distance between atoms and c, as given by Slater and Kirkwood (1931), is

$$c = \frac{3ekT}{4\pi\sqrt{m}} \frac{\alpha_1\alpha_2}{\sqrt{\alpha_1/N_2} + \sqrt{\alpha_2/N_2}} \tag{3.41}$$

where e is the elementary electric charge, k is the Boltzmann constant, m is mass of the electron, and N is the number of electrons in the outermost shell. Differentiating equation 3.40 with respect to r yields the force f as

$$f = \frac{6c}{r^7} \tag{3.42}$$

where r is the distance between atoms and n is the proportionality of force. For example, Casimir and Polder (1948) show that the force is proportional to r^{-8} for retarded van der Waals forces. The typical equation given in the literature for the attractive energy between two platelets is

$$V_A = -\frac{A}{48\pi}\frac{1}{d^2} = -\frac{A}{12\pi}\frac{1}{D^2} \tag{3.43}$$

In this instance $D = 2d$, and it is assumed that $\delta >> d$. To obtain the average attractive force per unit of the material (V_A), equations 3.39 and 3.43 must be differentiated for d and D, respectively, to give

$$V_A = \frac{A}{24\pi}\left[\frac{1}{d^3} + \frac{1}{(d+\delta)^3} - \frac{2}{(d+\delta/2)^3}\right] \tag{3.44}$$

and

$$V_A = \frac{A}{6\pi}\frac{1}{D^3} \tag{3.45}$$

These two equations are generally used for distances < 200 Å. For distances > 200 Å (Tabor and Winterton 1968), the attractive energy (V_A) would be R/D^4, where R is the retardation constant of the soil being used (see chapter 10). The value of parameter R (as used for V_A) for retarded attractive forces of platelet shapes (clay–air–clay) has been shown by various researchers to vary from 0.77×10^{-26} to 2.0×10^{-26} J m^{-1} (Tabor and Winterton 1968, and others). The lower value represents micas, and the higher value quartz. Values of A calculated

from theoretical analysis of coagulation measurements are 3.1×10^{-20} J for kaolinite, 2.5×10^{-20} J for illite, 2.2×10^{-20} J for montmorillonite, and 1.63×10^{-19} J for palygorskite (Novich and Ring 1984).

For spherical particles, the attractive energy due to van der Waals–London forces is

$$V_A = -\frac{A}{6}\left(\frac{2}{S^2-4} + \frac{2}{S^2} + \frac{S^2-4}{S^2}\right) \tag{3.46}$$

where A is the Hamaker constant, S is R/a which reduces to $2 + H/r$, R is the distance from sphere to sphere (center), r is sphere radius, and H is the minimum distance between spheres.

The Hamaker constant as normally written applies to the interaction between particles of a medium in a vacuum. For soils not in a vacuum, $A = A_{11} + A_{22} - A_{12}$, where A_{11}, A_{22}, and A_{12} are the Hamaker constants for particle–particle, water–water, and particle–water interactions. The Hamaker constant for mica–air–mica has been measured to range from 1.02×10^{-19} to 1.50×10^{-19} J (Tabor and Winterton 1968; Israelachvili and Tabor 1972). For a clay, A_{11} is approximately equal to that for mica–air–mica. Tabor and Winterton (1968) obtained 2.4×10^{-19} J for A_{22} while Verwey and Overbeek (1948) obtained 6×10^{-19} J. Assuming this latter value, A for a clay–water–clay system is approximately 10^{-19} J; assuming the value reported by Tabor and Winterton, A is about 2.0×10^{-19} J. Israelachvili and Adams (1978) obtained 2.2×10^{-20} J for the Hamaker constant using a mica–aqueous electrolyte solution of 10^{-1} to 10^{-3} mol KNO_3.

Schenkel and Kitchener (1960) derived an equation corrected for the effects of retardation when H < 150 Å,

$$V_A \approx -\frac{Ar}{12H}\frac{\lambda}{\lambda + 3.54\pi H} \tag{3.47}$$

and another when $H > 150$ Å,

$$V_A = \frac{Ar}{\pi}\left(\frac{2.45\lambda}{120H^2} - \frac{\lambda^2}{1045H^3} + \frac{\lambda^3}{5.62 \times 10^4 H^4}\right) \tag{3.48}$$

where λ is the wavelength of the London frequency. Both equations 3.47 and 3.48 are for equal spheres; equation 3.48 is accurate to about 5%.

QUESTION 3.9

What is the difference (if any) between van der Waals–London attractive force using equations 3.44 and 3.45? How does this compare to equation 3.46, assuming a spherical shape?

Total Potential Energy

The addition of attractive and repulsive forces yields the total potential energy (V_T) between charged particles (i.e., $V_T = V_R + V_A$). Since V_R depends on d, n_0, T, z, and δ, V_T is also a function of these. Forces of attraction (V_A) are negative; forces of repulsion (V_R) are positive and are usually expressed in J m^{-2}. Honig and Mul (1971) calculated the repulsive energy of a montmorillonitic soil under constant charge (σ) and constant potential (ψ) conditions (table 3.4). The repulsive energies in both instances are a function of κd and surface potential, assuming infinite distance of separation. The reduced repulsive energy between two parallel plane double-layer systems as they approach is determined by

$$V_R^{\psi} = \frac{64 n_0 kT}{\kappa}\gamma^2 e^{-2\kappa d} \tag{3.49}$$

TABLE 3.4 Repulsion Energy at Constant Potential (ψ) and Constant Charge Density (σ); $y_0 = 2 = e\psi_0/kT$

d^*	$W^{\psi\dagger}$	$1W^{\sigma\dagger}$
0.0	0.1358	∞
0.3	0.0873	0.1339
0.6	0.0522	0.0641
0.8	0.0365	0.0417
1.0	0.0253	0.0277
1.2	0.0174	0.0185

Source: Honig and Mul (1971).
$^*d = (\kappa/2)H_0$, where H_0 is the shortest distance between 2 plates.
$^\dagger W = (1/b)V_R; b = 64n_e kT/\kappa$ (J m^{-2}).

(Adamson 1990), where

$$\gamma = \frac{e^{y_d/2} - 1}{e^{y_d/2} + 1} \tag{3.50}$$

and κ is the Debye kappa. Equation 3.50 applies when surfaces are far apart, the potential midway between the plates is small, and there is weak interaction.

This repulsion plays a major role in determining colloidal stability against flocculation. Irving Langmuir (1881–1957) stated in 1938 that the total energy acting on the parallel planes may be regarded as the sum of an osmotic pressure force and an electrical field (Derjaguin and Churaer 1978). Total energy must be constant in the space between the parallel planes, and because the field $d\psi/dx$ is zero at the midpoint, total energy is given by the net osmotic pressure at that point. When the potential is large, the osmotic pressure, P, may be determined by

$$P = \frac{\pi}{2} D \left(\frac{kT}{ed}\right)^2 \tag{3.51}$$

Quite often, van der Waals–London forces of attraction are balanced by the electrical double-layer repulsion, such as in the flocculation of lyophobic colloids. In a colloidal solution, referred to as a sol, the charged particles will experience both van der Waals–London forces of attraction and double-layer repulsion. The balance of these two forces will determine the rate and ease of flocculation. For solutions of low ionic strength (measured by κ), the double-layer repulsion is very large, except at small separations. However, as κ is increased, a limiting condition of net attraction at all distances is reached (Adamson 1990). At a distance of separation x, almost equal to particle diameter, a critical region of the κ value is reached in which a small potential minimum of about $(1/2)kT$ occurs.

The preceding discussion demonstrates why increased ionic strength in a solution increases flocculation. The approximate net potential for a sol can be expressed, beginning with equation 3.49, as

$$V_R^{\psi} = \frac{64n_0 kT}{\kappa} \gamma^2 e^{-2\kappa d} - \frac{\left(\frac{1}{12}\pi\right)A}{x^2} \tag{3.52}$$

Adamson (1990) stated that if rapid flocculation is taken to indicate that no barrier exists, $V_R^{\psi} = 0$ and $dV_R^{\psi}(x)/dx = 0$ for some value of x. As a consequence, the ionic solution

concentration at which rapid flocculation will occur may be found from the following equation.

$$n_0 = \frac{2^7 3^2}{\exp(4)} \frac{\varepsilon^3 k^5 T^5 \gamma^4}{(ze)^6 A^2} \tag{3.53}$$

Thus, there is a straightforward relation between the flocculating concentration and the double-layer potential. Since z is valence, which typically has values of 1, 2, or 3, the concentration of ions of low valence (1–2) increases as double-layer potential increases. For large values of y_d (large values of z and/or ψ_0), concentration is insensitive to values of potential, and it approaches a limiting value because γ approaches unity. This holds for the Schulze-Hardy rule for the effect of valence type on the flocculating ability of ions. Because of the increased tendency for specific adsorption of ions with greater charge, the ability to flocculate depends on the reduction of potential and double-layer thickness. For a more detailed discussion, the reader is referred to Adamson (1990) and Verwey and Overbeek (1948).

QUESTION 3.10

In question 3.3, you were given a surface potential of 75 mV. As a comparison with the Gouy–Chapman theory, calculate the surface potential of the same clay material used in question 3.3 from $\psi_0 = \sigma 4\pi/\varepsilon\kappa$, (you will have to first compute κ).

Non-DLVO Forces

The stability of colloids is affected by forces other than those of DLVO origin, including hydration repulsive forces, hydrophobic attractive forces, and steric forces. During flocculation, particles are closely attracted; ions associated with these particles require a partial loss of their hydration for flocculation to occur. This process requires repulsive forces known as hydration forces, which can be appreciable in aqueous colloidal systems. Hydration forces partially negate van der Waals–London attractive forces, allowing dispersion of soil to occur more easily by reducing the electrolyte concentration. As water surrounds a particle, hydrogen bonding assures a well-structured affect. Normally, as water covers a particle, repulsive forces between particles help force them apart, but in the absence of water, hydrophobic attraction between colloidal surfaces occurs that is stronger than van der Waals–London forces and extends away from the surface. However, Adamson (1990) indicates that van der Waals attraction of water to itself seeks to exclude hydrophobic particles, making them stick together more tightly than they would due only to their own forces. Steric forces, associated with the adsorption of minute amounts of organic compounds on the edges of clay particles and the surfaces of sesquioxide compounds, can lead to charge reversal in the areas of adsorption. This can promote dispersion by preventing interaction between oppositely charged surfaces.

Limitations of the DLVO Theory

The repulsive and attractive forces between double layers in the DLVO theory are calculated considering ions as point charges. Research by Israelachvili and Adams (1978) and Ducker, Senden, and Pachley (1991) has shown good agreement with calculations based upon the DLVO theory. The theory works well when distance between particles is great enough, usually $>$ 30–40 Å, that the magnitudes of ions present can be ignored. The theory fails at shorter distances from the surface. This is partially a result of non-DLVO forces and capillary effects, as well as the presence of bivalent ions that are more likely to approach the colloid

surface than monovalent ions. Generally, the electrical intensity or potential at points midway between two particles, where the distance from the charged surface is greater than the average distance between adjoining charges on the surface, prevails in the majority of soils. This makes use of the DLVO theory attractive.

3.5 ION EXCHANGE

Ion exchange refers to a reversible process in which both cations and anions are exchanged between solid and liquid surfaces. The active fraction of soils in which ion exchange occurs consists of clay, colloidal organic matter, and silt. Positively charged ions are attracted to the surface of negatively charged particles within soil. Charges in organic matter and humic acid arise from —COOH and —OH groups. The charge associated with ion–surface interaction arises from isomorphous substitution, and from ionization of hydroxyl groups attached to silicon atoms at the lattice defects (i.e., broken edges) of tetrahedral planes. This substitution is balanced by ion exchange between the layers, and charge is usually balanced by the potassium ion. The substitution is generally in the form of a monovalent ion exchanging for a divalent ion in a mass action approach, that is,

$$CaX_2 + 2K^+_{(aq)} \rightleftharpoons 2KX + Ca^{2+}_{(aq)} \tag{3.54}$$

Here, X represents the negatively charged surface assuming an adequate number of available exchange sites. Mass action can be described as

$$K_c = \frac{(KX)^2(Ca^{2+})}{(CaX_2)(K^+)^2} \tag{3.55}$$

where K_c is the exchange equilibrium constant and the parentheses are activities.

Additional reactions of exchange include the following.

$$\begin{gathered} CaCO_3 + Sr^{2+} \rightleftharpoons SrCO_{3(s)} + Ca^{2+} \\ Fe(OH)_{3(s)} + HPO_4^{2-} + 2H^+ \rightleftharpoons FePO_{4(s)} + 3H_2O \end{gathered} \tag{3.56}$$

There are many such reactions; however, these will suffice for purposes of illustration. If divalent ions exchange for monovalent ions, only half as many will be needed to balance the charge. This is a good example of the Gouy theory, which predicts a greater concentration of divalent ions in the double layer than monovalent ions, and which agrees with experimental data.

Cation Exchange Capacity

The ability of soils to exchange cations is referred to as the cation exchange capacity (CEC), and is expressed as the quantity of exchangeable cations in milliequivalents per 100 g of oven-dry media. Ion exchange occurs entirely within the double layer of the soil solution or suspension liquid. In figure 3.4, the ion exchange capacity corresponds to the area marked as σ^+, which is the charge due to a surplus of cations, whereas σ^- is the charge due to a deficiency of anions. Because ions are preferentially adsorbed electrostatically due to isomorphous substitution and ionization, CEC is pH dependent; that is, charge increases with increasing pH. Since surface mechanisms are not explained by simple CEC models, equations used here are derived from a basic understanding of thermodynamic properties of ions that are independent of process.

Montomorillonitic clays allow water to penetrate into the interlayer spaces and are high-swelling clays (Low 1979). Water penetrates these interlayer spaces due to the difference in

osmotic pressure between the interlayer space and the surrounding solution, and interlayer spacing becomes a function of the hydration tendency of the counterions and interlayer forces. As the hydration of the counterion increases, swelling results in increased distance of the interlayers. Half as many divalent ions as monovalent ions are required to balance the charge, so the osmotic pressure between interlayer and solution is reduced, and less swelling will be observed for a solution of divalent ions than if a monovalent ion (such as Na^+) were present.

If coulombic interaction between counterions is less than the ion-induced dipole interactions between counterions and water molecules, the affinity of ions for the exchangeable surface will follow the Hofmeister series (Sposito 1984):

$$Cs^+ > K^+ > Na^+ > Li^+ \tag{3.57}$$

and

$$Ba^{2+} > Sr^{2+} > Ca^{2+} > Mg^{2+} \tag{3.58}$$

(In other words, the ion of larger hydrated radius is replaced with an ion of smaller hydrated radius.)

Sodium Adsorption Ratio

The Gapon equation is used extensively in understanding the exchange of Na^+ for Ca^{2+} in saline soils. The activity of individual ions on the surface is equal to the ions' equivalent fraction there; thus, the Gapon approach to cation equilibria may be written as

$$Ca_{1/2}X + Na^+_{(aq)} \rightleftharpoons NaX + \frac{1}{2}Ca^{2+}_{(aq)} \tag{3.59}$$

(Mott, 1988). Notice the close similarity of the Gapon approach to the commonly used mass action approach, (equation 3.54). Using the Gapon approach, the equilibrium constant is expressed by

$$K_c = \frac{(NaX)\sqrt{(Ca^{2+})}}{(Ca_{1/2}X)(Na^+)} \tag{3.60}$$

Thus, the Gapon constant (K^G) may be expressed using solution concentrations instead of activities as

$$K^G = \frac{\sqrt{[Ca^{2+}]}}{[Na^+]}\frac{[NaX]}{[Ca_{1/2}X]} \tag{3.61}$$

Saline soils usually contain considerable amounts of Mg^{2+}, which is assumed to exchange in a manner similar to Ca^{2+}, and which has the following Gapon relationship expressed in equivalent units.

$$\frac{[NaX]}{[(Ca + Mg)X]} = K^G\frac{[Na^+]}{\sqrt{\frac{[Ca^{2+} + Mg^{2+}]}{2}}} \tag{3.62}$$

Generally, the ions of significance in saline soils are calcium, magnesium, and sodium. Considering this, equation 3.62 describes the sodium adsorption ratio (SAR), which is a characteristic of ions dissolved in soil solution; that is, a ratio for soil extracts and irrigation water used to express the relative activity of sodium ions in exchange reactions with soil. The SAR may be expressed by

$$SAR = \frac{[Na^+]}{\sqrt{\frac{[Ca^{2+} + Mg^{2+}]}{2}}} \tag{3.63}$$

The exchangeable sodium percentage (ESP) is the degree of saturation of the soil exchange complex with sodium. ESP = [NaX/CEC] × 100; or, for a soil that is in equilibrium with the irrigation water that has been applied,

$$\text{ESP} = \frac{\dfrac{100\ \text{SAR}}{K^G}}{1 + \left(\dfrac{\text{SAR}}{K^G}\right)} \tag{3.64}$$

The SAR is an indicator of the suitability of water for irrigation purposes on already irrigated land, or for irrigation during land reclamation. The ESP was originally used as the main criterion for measuring excessive sodium levels in soils, but more emphasis has now been placed on the SAR. This is probably due to the fact that the ESP of surface soil can be predicted reasonably well from the SAR of applied water, because surface soil is being equilibrated with the applied water at each application. When the ESP is initially high, puddling of soils can decrease the percolation rate to the point that an extended period of time is required for land reclamation using water with a low SAR value. The ESP measurement in such cases can indicate how much lime or gypsum is necessary to acquire adequate tilth to begin reclamation. For a more detailed discussion of the SAR and ESP, the reader is referred to Bresler, McNeal, and Carter (1982).

3.6 HYDRATION AND SHRINKING OF CLAYS

Hydration

The imbibition of water by a clay is sometimes accompanied by an increase in volume. This phenomena is termed swelling, which is a macroscopic manifestation of expansion between clay layers caused primarily by an increase in volumetric water content. The crystal layers of some clays, such as kaolinite are bound together by hydrogen bonding; whereas illite layers are bound by potassium within layers (Hunter and Alexander 1963). Both of these elements cause very tight bonding, making it virtually impossible for liquid to enter between the layers. Consequently, hydration of these clays results in little or no swelling. In contrast, layers of montmorillonite clay are bound by cations that exchange easily for other cations in the surrounding aqueous solution. As a result, water molecules can be attracted to the cations and can be allowed to enter between the layers, resulting in a high swelling ability. As water enters an initially dry montmorillonite, the energy of hydration due to ion–dipole electrostatic attractions causes water to bond to cations, increasing the effective size of the cation. If this cation is between platelets, the platelets will normally be pushed apart, allowing other molecules to enter between them. This type of swelling is due to short-range interactive forces between the layers of expanding media, or between the planar surfaces of individual mineral crystals.

The influence of salt on water imbibition by clays varies according to the lyotropic series (Sumner and Stewart 1992). When large amounts of salts are either present in or added to soil, "salting out" may occur (precipitation of salt). Good examples of this occur in soils in the western United States and the arid Middle East. The lyotropic series for cations is

$$Mg^{++} > Ca^{++} > Sr^{++} > Ba^{++} > Li^{+} > Na^{+} > K^{+} > Rb^{+} > Cs^{+} \tag{3.65}$$

and for anions is

$$\text{Citrate}^{---} > \text{Tartrate}^{---} > SO_4^{-} > C_2H_3O_2^{-} > Cl^{-} > NO_3^{-} > ClO_3^{-} > I^{-} > CNS^{-} \tag{3.66}$$

The anions citrate, tartrate, sulfate, and acetate inhibit swelling; whereas chloride, nitrate, and so on favor water imbibition. Swelling depends upon the nature and pH of the electrolyte, as well as on the anionic species present. If we assume that the soil is at equilibrium before the addition of an electrolyte, the swelling pressure is given by

$$P_s = \frac{\Delta\mu}{w_s} \tag{3.67}$$

where P_s is the swelling pressure, $\Delta\mu$ is the difference in chemical potential between the outer and inner solution, and w_s is the specific volume of water in the sample (cm^3). Imagine clay platelets separated by distance $2d$ (as in figure 3.6), with a chemical potential of μ_i between the two plates and a chemical potential of μ_o in the outer aqueous solution surrounding the two plates. Initially,

$$\mu_o = \frac{-RT \sum n_i \pi_i w_s}{1000} \tag{3.68}$$

where n_i is the molarity of solute i and π_i is its osmotic coefficient. After adding an electrolyte, equilibrium is disturbed and μ_o changes to a new concentration μ_o', which may be given by

$$\mu_o' = \frac{-RT \sum n_i' \pi_i' w_s}{1000} \tag{3.69}$$

Considering that, initially, $\mu_o = \mu_i$, then $\Delta\mu = \mu_o' - \mu_i$, which may be found by

$$\Delta\mu = \frac{RT \sum (n_i\pi_i - n_i'\pi_i')w_s}{1000} \tag{3.70}$$

This can be calculated if the change in concentration of the outer solution is known.

Thermodynamically, soil absorbs water until the partial molar free energy of the water adsorbed equals that of water in the equilibrium solution. As the particles are hydrated, the ions in the diffuse layer between the two platelets reduce the free energy of the free water. This causes diffusion of water from the outer aqueous solution into the inner solution between the particles. Consequently, as water is absorbed, the platelets push apart, exhibiting a swelling pressure. The platelets will continue to push apart until the increase in the free energy of water (due to hydraulic pressure) equals the decrease in free energy of water (caused by the higher ionic concentration between the particles when compared to the external solution). Mathematically, this is described by

$$V\,\Delta P = \Delta F = -RT \ln \frac{M_i}{M_o} \tag{3.71}$$

where V is the molar volume of water (18 $cm^3\ mol^{-1}$), P is pressure (dynes cm^{-2}), F is free energy (ergs mol^{-1}), T is absolute temperature, M_i is the mole fraction of water in the inner solution, and M_o is the mole fraction of water in the outer solution. Then, for dilute solutions ($M < 0.1$)

$$-\Delta M_{\text{solute}} \approx \ln \frac{M_i}{M_o} \tag{3.72}$$

Considering this, equation (3.67) can be rewritten as

$$\Delta P = \frac{RT}{V} \Delta M_{\text{solute}} \tag{3.73}$$

Also, because the ratio of M_{solute} per molar volume of water ($cm^3\ mol^{-1}$) is approximately equal to the difference in concentration of solutes (n_i) in mol cm^{-3}, then

$$\Delta P = RT \sum (n_i - n_{io}) \text{ ergs cm}^{-3} \tag{3.74}$$

where n_i is the concentration of ionic species i (mol cm^{-3}), and n_{io} is the concentration of ionic species in the outer solution (which follows Boltzmann's law of distribution for cations and anions, as given in equation 3.28). Substituting equation 3.28 into equation 3.74, the osmotic pressure difference between any point where the potential is ψ_d and a point in the equilibrium solution where the potential is zero can be written as

$$\Delta P = RTn_o(e^{y_d} + e^{-y_d} - 2) \tag{3.75}$$

which leads back to equation 3.31:

$$P_e = n_0kT(e^{-y_d} + e^{y_d} - 2) = 2n_0kT[\cosh(y_d) - 1]$$

The general relation between potential and anion and cation concentration for overlapping double layers is given in figure 3.8.

At the midpoint d, between the two platelets, $d\psi_d/dx = 0$ ($\psi_d \neq 0$), net dipole attraction of water molecules to either particle surface is essentially zero. Letting $x = y_d$, the difference between osmotic pressure at the midpoint, where $d = x_d$ (d is distance, x_d is dimensionless), and that in the equilibrium solution is a good measure of swelling pressure. From this, the swelling pressure can be calculated as

$$\Delta P = 2RTn_0(\cosh(y_d) - 1) \tag{3.76}$$

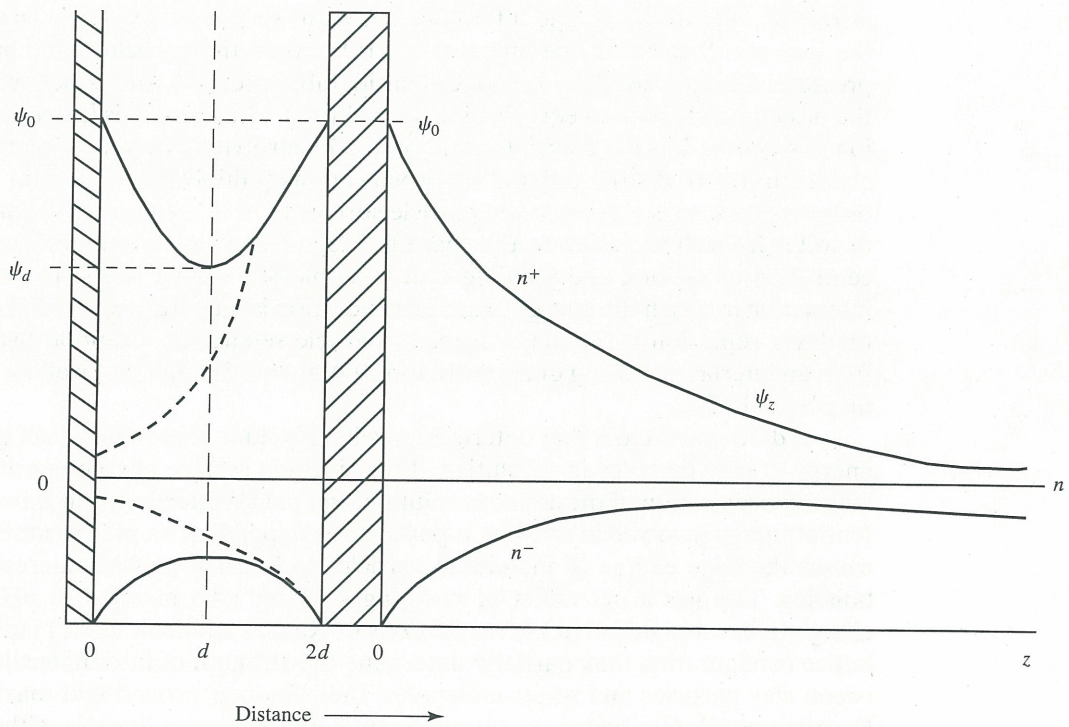

Figure 3.8 Representation of overlapping double layers, showing electrical potential (ψ) and cation and anion concentration ($n^{+/-}$). Data from Kruyt (1952)

TABLE 3.5 Relation of Swelling to Clay Mineral Type and Exchangeable Cations

	Swelling $cm^{-3} g^{-1}$					
Clay Mineral	H^+	Li^+	Na^+	K^+	Ca^{2+}	Ba^{2+}
Beidellite	0.81	4.97	4.02	0.50	0.91	0.85
Halloysite	0.05	—	—	—	—	—
Montmorillonite	2.20	10.77	11.08	8.55	2.50	2.50

Montmorillonite has very prominent swelling properties that are due mainly to interparticle water interaction. Table 3.5 demonstrates swelling properties in the lyotropic series for both beidellite and montmorillonite clays. The hydration energy of clays is cation dependent. Likewise, the intake of water varies considerably with the nature of the clay. It is initially very rapid but slows with time. Typical clays take about one to three days to become completely hydrated, while bentonite may take up to one week. For some clay minerals, swelling decreases with diminishing hydration, in the following order.

vermiculite > montmorillonite > beidellite > illite > halloysite

Another manner of swelling, caused by hydration, is osmotic swelling. Osmotic swelling is caused by the presence of hydrated ions that surround the hydrated surface of the particle in the diffuse electrical double layer, and that are dissociated from the surface. At this juncture, the osmotic forces are in equilibrium with the van der Waals–London forces of attraction, due to the charge difference between the particle and exchangeable ions. Since the ions are dissociated, the influx of water between the particles is a function of osmotic pressure. Osmotic swelling generates considerable pressure, and is believed to function by the principles of Donnan equilibrium: $X^2 = Y(Y + Z)$, where X is the concentration of each ion in solution, Y is the concentration of each electrolyte between the platelets, and Z is the concentration of dissociated and adsorbed cations (Ghildyal and Tripathi 1987). Generally, osmotic pressure is greater at the particle surface than in the outer solution. Thus, the influx of water from the solution to the space between the platelets counteracts the greater concentration of cations, and swelling occurs. Osmotic swelling is due to long-range particle interaction in which the energy of surface hydration is inoperative, and diffuse electrical double layer repulsion is the major force of particle separation. Osmotic swelling takes place from an interlayer spacing of about 10 to 120 Å at equilibrium; the swelling pressure induced may be > 1 MPa.

Additional factors that determine swelling include those that affect the total potential energy of clay particles in a solution. These include surface charge density, counterion valence, concentration of the aqueous solution, and pH (Winterkorn and Baver 1934). Total potential energy involved in swelling is particularly dependent on pH, because a decrease in pH causes the edge charge of individual particles to become positive, increasing edge-to-face bonding. This has a net effect of reducing swelling. (An increase in pH causes the edge charge to become negative.) Investigations of Ravina and Low (1972) indicate that crystal-lattice configuration may partially determine the strength of intermolecular interaction between clay particles and water molecules. Their findings proved that maximum swelling of Na-montmorillonite under no external constraint decreases linearly with a subsequent increase in the dry-state b dimension (figure 3.9). They also found that the magnitude of the b

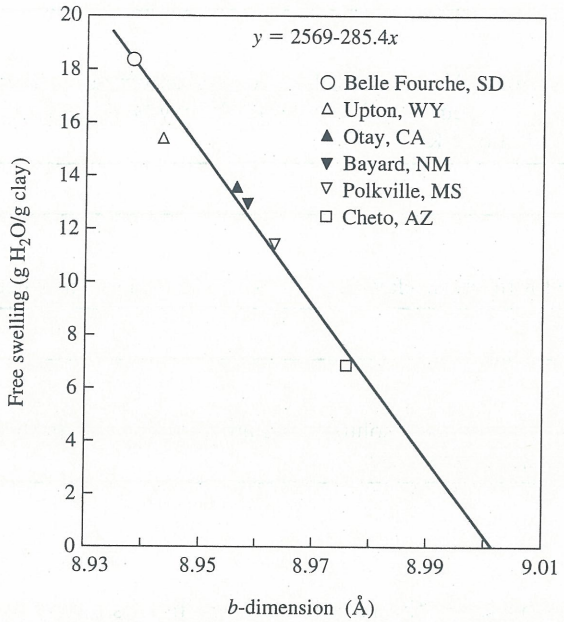

Figure 3.9 Swelling of clays versus the *b*-dimension; data from Ravina and Low (1972)

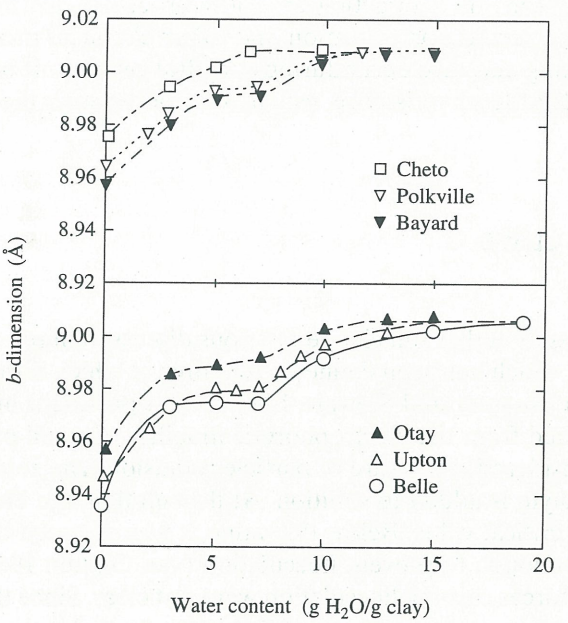

Figure 3.10 Relation between the *b*-dimension and soil water content; data from Ravina and Low (1972)

dimension increases incrementally with water content until a final *b* dimension is reached (figure 3.10). The *b* dimension can be defined as the *b* axis, and is the characteristic width in relation to the depth (*a*-dimension, or axis) and height (*c*-dimension, or axis) of the clay molecule; the *b* dimension has also been defined as the interlayer spacing or basal spacing—the distance between the lowest sheet of one layer and the equivalent sheet in the layer above. Further details about the *b* dimension are given in Grimshaw (1971).

QUESTION 3.11

What is the swelling pressure for a Na-montmorillonitic clay, assuming that $w_s = 1$, $n_i = 10^{-4}$ M, $n_i' = 10^{-2}$ M, $\pi_i = 2$, $\pi_i' = 2$, $v_s = 1$ g cm^{-3}, and $T = 25$ °C? It may be assumed that NaCl is the electrolyte and that $R = 0.082$ atm L mol^{-1} K^{-1}.

QUESTION 3.12

What is the swelling pressure for the same clay if equation 3.73 is used for the calculation parameters?

QUESTION 3.13

What is the potential energy between a soil solution and an adjoining clay particle where $d = 2.6$ Å, $\varepsilon = 78.8$, and σ is as calculated in question 3.3?

Shrinking

The process of shrinking is basically the reverse of swelling. As a clay loses water, the distance between platelets collapses (due to dehydration) as the medium approaches its original volume before it was wetted up. This indicates a return of the interlayer spacing to about 2.6 Å for 2:1 clays. However, the interacting chemical processes are not necessarily reversible as the medium dehydrates; precipitation and other chemical processes may occur during dehydration. Cracking may also occur during dehydration in some soils where lines of cleavage develop at points of least resistance, usually coinciding with the areas of greatest water content.

3.7 FLOCCULATION AND DISPERSION OF CLAYS

Flocculation

Flocculation of clays results directly from charge relations discussed in previous sections. The term *critical zeta potential,* which has been defined as the time at which flocculation will occur within a colloidal solution (Sumner and Stewart, 1992), is still prevalent in textbooks. While the zeta potential is obtained from the electrophoretic mobility of a soil particle, the magnitude of the mobility is considered a measure of particle repulsion. The zeta potential usually decreases when an electrolyte is added to solution. At flocculation, the electrolyte was considered to have reached a critical value. Below this value, it was assumed that particle repulsion was no longer strong enough to prevent flocculation (van Olphen 1963). At the time of that writing, the nature of forces causing flocculation were not clear. Since that time, it has become clear that the primary force or framework of the zeta potential is the slipping plane.

Because the position of the slipping plane is not known, the zeta potential is the electric potential at some unknown distance from the surface of the double layer. As a result, the zeta potential is not equal to the surface potential, but somewhat comparable to the Stern potential. It is not surprising, therefore, that a relation exists between the stability of colloids and the magnitude of the zeta potential. Due to its ill-defined character, the zeta potential is not useful as a quantitative criterion of colloidal stability.

As colloids lose their stability, they tend to flocculate, which occurs when attractive forces overcome repulsive forces. The flocculation concentration, F_c, at which attractive

forces dominate and flocculation will occur, is described mathematically by

$$F_c = \frac{K\left[\tanh\left(\frac{ze\psi_0}{4kT}\right)\right]^4}{A^2 z^6} \tag{3.77}$$

(Sumner and Stewart 1992), where F_c is the flocculation concentration value (m mol/L), z is counterion valence, e is the electronic charge, ψ_0 is the electric potential at the surface, A is the Hamaker constant, k is the Boltzman constant (1.38×10^{-23} J K^{-1}), and K is a constant (8×10^{-36} J^2 L^{-1} or 8×10^{-22} ergs^2 L^{-1}—assumed constant for most soil solutions). From this equation, the influence of ionic valence on the precipitating effect of the ion can be seen. This effect is known as the Schulze–Hardy rule, which denotes the dependence of F_c on z^{-6}, indicating that ionic charge has a dominant effect on flocculation. According to this rule, flocculation values range from 25 to 150 m mol L^{-1}, 0.5 to 2 m mol L^{-1}, and 0.01 to 0.1 m mol L^{-1} for monovalent, divalent, and trivalent ions, respectively. Consequently, ions such as Ca^{2+} or Ba^{2+} have a much greater effect on flocculation of clays than K^+. As ions of opposite charge than that of clay particles prevail, the numerical value of the potential within the slipping plane and, thus, the zeta potential, will change. Positive ions increase potential in the slipping plane and negative ions decrease it. When potential in the slipping plane decreases, the velocity of individual particles slows and flocculation takes place. Within the electrical double layer, ions effective in precipitation are adsorbed onto the solution side of the fixed part of the double layer (see figure 3.4).

Rengasamy and Sumner (forthcoming) have derived a factor based upon the ratio of the first to the second ionization potential of the cation and its valence. They have suggested that hydration and flocculation effects depend on this factor, termed the flocculative power. The flocculative power $\approx 100(I_z/I_{z+1})^2 z^3$, where I_z is the zth ionization potential, and z is the cation valence.

As an example of the effect of ionic valence on the zeta potential, consider a soil system (colloidal in nature) that is typically negatively charged. The addition of a monovalent electrolyte will increase the zeta potential (BC in figure 3.11). If excess electrolyte is added, the thickness of the double layer will tend to collapse due to a decrease in charge density (Rengasamy 1983); as a result, the zeta potential will decrease as well. In this situation the

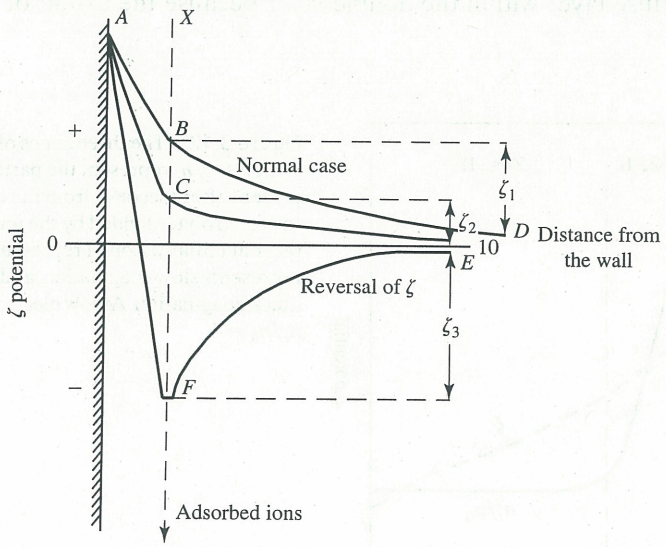

Figure 3.11 Effect of ionic valence on zeta potential

cations will accumulate near the particle surface (*AB* in figure 3.11) or rigid layer (also see figure 3.4), which is the solution side of the electrical double layer. The decrease in zeta potential is shown by line *CD* in figure 3.11. As the valence of the ion in the added electrolyte increases, the smaller the quantity of electrolyte required to effect the same changes in zeta potential. A continual addition of electrolyte will result in a reversal of zeta potential sign, due to surface charge neutralization or decreased electrical double layer thickness. The double layer can actually collapse and reform with a reversed charge (*FE* in figure 3.11).

There are essentially three stages of flocculation (figure 3.12): **(1)** a stable colloidal suspension (zone I); **(2)** slow flocculation (zone II); and **(3)** fast flocculation (zone III). For low concentrations of electrolytes ($n_t/n_0 = 1$), the suspension is stable (i.e., dispersed). Collision of particles in this stage does not form a stable consolidation; however, the zeta potential changes appreciably. During the second stage a slow flocculation occurs because the zeta potential incrementally decreases in a uniform manner while n_t/n_0 falls rapidly. This implies that collisions rise from 0 to 1 in a small range of electrolyte concentrations. During the third stage, n_t/n_0 remains constant while zeta potential decreases. During this stage, collisions between particles are more effective and the suspension becomes unstable (flocculates). Thus, flocculation may occur very rapidly or slowly, dependent on both Brownian motion and particle interaction. For flocculation to occur, the net repulsive forces within the system must decrease. Usually, the smaller particles will flocculate first, since collisions between large and small particles are occurring and the number of small particles is likely to decrease with respect to visible changes in large particles. Arid zone soils contain large amounts of salts that affect both flocculation and dispersion. If an applied salt contains the same cation with which a clay soil is saturated, compression of the double layer will occur, lowering the net negative charge of the system, reducing the repulsive capacity and, thus, inducing flocculation. If the applied salt contains a different cation, compression of the double layer will still occur; however, ion exchange will also occur.

Dispersion

In dispersion (occasionally referred to as deflocculation), the addition of monovalent cations causes increased hydration of the clay micelles, which causes particles to repel each other. In this instance, the zeta potential is increased. The presence of monovalent cations results in a more extensive diffuse layer within the double layer because the extent of the double layer

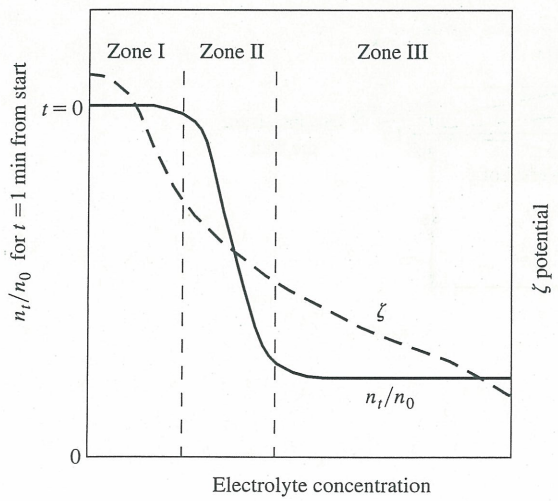

Figure 3.12 The three zones of flocculation. The symbols n_t/n_0 represent the particles per unit volume present after t seconds from the time of addition of the electrolyte, divided by the number of particles present initially. Zone I represents a stable sol, zone II represents slow coagulation, and zone III represents quick coagulation. At low electrolyte concentration, $n_t/n_0 = 1$

varies inversely with cation charge (valence), as described by the Schultze–Hardy rule. As this extensive diffuse layer develops around each particle, it prevents adjacent particles from approaching; thus, they remain as separate particles. In effect, dispersion is the opposite of flocculation as just discussed. In particle size analysis, dispersion is accomplished by mechanical shaking and the addition of a chemical dispersing agent, because most soils are not easily dispersed. However, some soils (such as those found in the southeastern United States) require very little mechanical energy to disperse, and actually have been found to disperse readily by the kinetic energy supplied by rainfall. Miller and Radcliffe (1992) surveyed thirty-five topsoils in the southeastern United States and discovered that a majority contained more than 50% of their total clay content in a water-dispersible form. Soils in the western United States are also easily dispersed, consequently these soils exhibit low infiltration rates. Dispersion greatly affects the sealing and crusting of soils, and hydraulic conductivity (which will be discussed in greater detail in chapter 8).

QUESTION 3.14

Determine the value of F_c that will result in flocculation for a montmorillonite soil that has NaCl as a background electrolyte. Assume $T = 25\ ^\circ C$, NaCl = 0.017 M, $\varepsilon = 78.8$, $\psi_0 = 25$ mV or 0.025 J/C, $e = 4.803 \times 10^{-10}$ esu ion^{-1}, $z = 1$, $k = 1.381 \times 10^{-16}$ erg ion^{-1} K^{-1}, $A = 2.2 \times 10^{-13}$ erg, and $K = 8 \times 10^{-36}$ J^2/L or 8×10^{-22} erg^2/L.

3.8 HUMUS IN SOILS

Humic and Fulvic Acids

The organic fraction of soil is composed of living organisms and their partially to completely decomposed remains. The term organic matter refers to the heterogeneous mixture of products resulting from chemical and microbial transformation of organic animal and plant debris. This transformation is known as the humification process and gives rise to humus. Humus is a mixture of variously transformed organic debris, which has a high resistance to further decomposition by microbes, and bears little resemblance to structures from which it was derived. Generally, humus is classified into two major groups: amorphous, polymeric humic substances, which are usually differentiated by solubility characteristics as either humic acids, fulvic acids, or humins (these are usually brown in color); and compounds such as polysaccharides, polypeptides, and altered lignins, which can be synthesized by microorganisms or may occur from modifications of comparable compounds from the original organic debris.

Humic and fulvic acids and related constituents are plentiful in soils, as well as ground and surface waters (Stumm and Morgan 1981; Kumada 1987; Oades 1989). Physically, these substances sometimes appear as yellow to black polyelectrolytes. Humic substances occurring in soil and natural waters have similar characteristics. They have large specific surface areas (900 m^2 g^{-1}) and high CEC (1500 to 3000 meq kg^{-1}; Schnitzer 1976). The development of adequate extraction and fractionation processes to isolate separate humic compounds has been difficult. Consequently, humic and fulvic acids, although known to give specific characteristics to soil and natural waters, have been hard to identify, and a satisfactory method for determining the occurrence of humic and fulvic acids in various environments has not been established. Humic substances have molecular weights ranging from approximately 300 to 300,000; in contrast, fulvic acids are relatively low in molecular weight, and contain higher O_2 but lower carbon contents. Fulvic acids also contain more acidic (COOH) functional groups. The OH groups associated with humic and fulvic acids are presumed to be phenolic. Both humic and fulvic acids contain a variety of carboxylic and phenolic functional (hydrophilic)

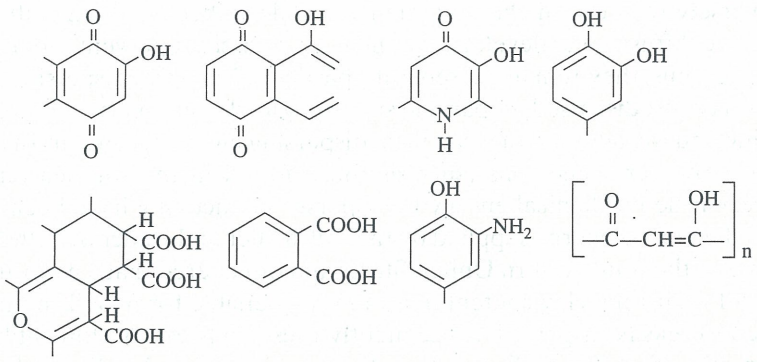

Figure 3.13 Various functional groups associated with humic substances

groups and aliphatic and aromatic moieties, which convey hydrophobic properties to these substances (see figure 3.13). Humic fractions within soil are believed to represent a system of polymers which systematically vary in pH, elemental content, molecular weight, and degree of polymerization (Stevenson 1982a, 1985). Humins, on the other hand, are believed to consist of humic acids that are so closely bound to mineral matter that the two cannot be separated. Soil contents of humic and fulvic acids vary by depth, climate, and geography (Thurman 1985b). Forest soils such as alfisols, spodosols, and ultisols generally are high in fulvic acids, whereas grassland soils such as mollisols are high in humic acids.

Humic substances in soils usually occur in insoluble forms and are bound in three ways: as insoluble macromolecular complexes; combined with clay minerals through polyvalent cations, hydrogen bonding, and van der Waals–London forces; and as macromolecular complexes bound together by cations such as Ca^{2+}, Al^{3+}, and Fe^{3+}. Macromolecular complexes generally occur in organic rich soil, such as peats and organic rich sediments, where clay–metal complexes are present in low amounts compared to humus substances. For forest soils such as spodosols, significant amounts of aluminum, iron, and organic matter have been mobilized and transported deeper into the profile in the B horizon. Consequently, this horizon has an abundant supply of fulvic acids that can be separated from the sesquioxides by mild extractants.

Because clays and organic colloids are normally negatively charged, humus substances associated with bi- and trivalent ions can form clay–humate complexes; the cation satisfies the surface charge, thus linking the colloids together. The trivalent cations form coordination complexes with humic substances in which bonding is very strong. In these instances, extraction and fractionation is difficult. Typically, in soils with organic matter, the CEC is proportional to the amount of organic matter present. About 30–90% of the total CEC of soils is a result of the organic fraction of the media.

The formation of stable complexes with polyvalent cations facilitates the mobilization, transport, segregation, and deposition of trace metals in soils. Because organic complexing agents function as carriers, trace metals found in soils normally occur in organically bound forms. However, not all natural occurrence of trace metal cycling is attributable to humic substances. A schematic denoting organic matter–trace metal interactions is given in figure 3.14. The ability of humic substances, R, to form complexes with metal ions is due to the functional groups present, such as COOH, phenolic OH, enolic OH, and C=O structures. Examples of these include

$$R—\overset{\overset{O}{\|}}{C}—OH\cdots O=C—O.M. \tag{3.78}$$

where R is a polyanionic humic colloid, C is carbon, O is oxygen, OH is the hydroxyl group, and O.M. is organic matter (Hayes and Swift 1978).

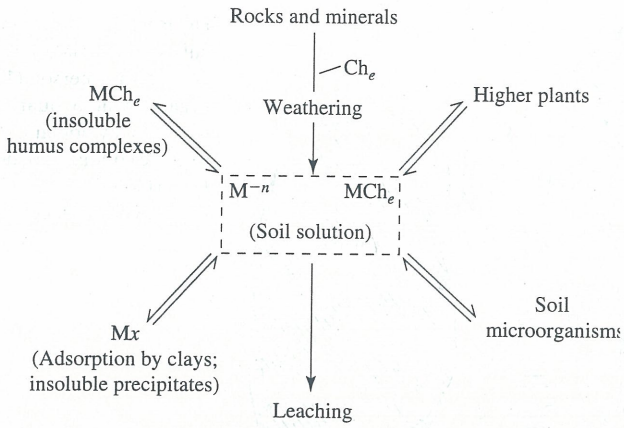

Figure 3.14 Organic–trace metal interactions of humic substances

Many instances occur in which soils exhibit hydrophobic characteristics. These are generally associated with dry spots on golf greens, burned forest areas, and citrus groves, and have been associated with coarse textured sands. This hydrophobic behavior has sometimes been attributed to fats and waxes coating the sand particles, as well as fulvic acids synthesized by fungi (Miller and Wilkinson 1977). This is a result of the effects of the humic substances on the contact angle of water on individual particles (which will be discussed in detail in chapter 5). Both humic and fulvic acids have been classified as hydrophobic substances, due to their adsorption onto resins with pH adjustment (low pH for acids and neutral pH for bases). Due to the characteristics of humic substances to convey hydrophobic properties, the hydrophobic interaction of humic and fulvic acids tends to accumulate at the particle–water interface. Additionally, adsorption is influenced by a coordinative interaction:

$$\equiv\text{Al—OH} + \text{RC}\begin{matrix}\overset{\overset{\text{O}}{\|}}{}\\ \underset{\text{OH}}{}\end{matrix} \rightleftharpoons \equiv\text{AlO—}\overset{\overset{\text{O}}{\|}}{\text{C}}\text{—R} + \text{H}_2\text{O} \tag{3.79}$$

Adsorption of humic substances is multicomponent; thus, the Langmuir equation cannot be used to calculate it, because this equation is based on a single adsorbate. During the adsorption of humic substances to particles, an interface fractionation occurs because larger molecules adsorb preferentially over smaller ones. Thus, the molecular weight of material in solution is lowered. In terms of ion transport (see chapter 10), immobilization and increased residence time within the soil system occurs. The kinetics of these reactions are controlled by diffusion or convection. As with sesquioxides in variable charged soils, humic acids adsorbed to particles alter their chemical properties and, thus, their propensity for metal cations. This adsorption (hydrated surface) can be described by

$$\text{S(H}_2\text{O)}_m + \text{X(H}_2\text{O)}_n \rightleftharpoons \text{SX(H}_2\text{O)}_a + (m + n - a)\text{H}_2\text{O}; \quad \Delta G^\circ_{\text{ads}} \tag{3.80}$$

Assuming ΔG° for hydration of the product is small, the free energy of adsorption is given by

$$\Delta G^\circ_{\text{ads}} = \Delta G^\circ_1 - \Delta G^\circ_{\text{solv}} \tag{3.81}$$

where ΔG°_1 is given as

$$\text{S(H}_2\text{O)}_m + \text{X} \rightleftharpoons \text{SX(H}_2\text{O)}_m \tag{3.82}$$

and $\Delta G^\circ_{\text{solv}}$ is given as

$$\text{X} + n(\text{H}_2\text{O})\,\Delta\text{X(H}_2\text{O)}_n \tag{3.83}$$

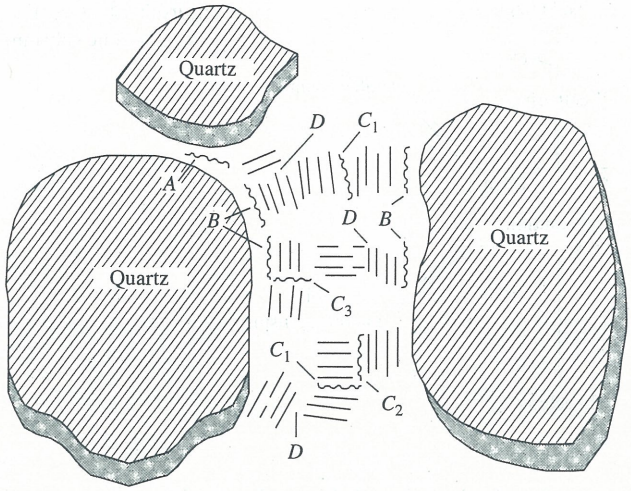

Figure 3.15 Amphipathic organic molecule self-association with particle surfaces; data from Emerson (1959). (A) Quartz–organic colloid–quartz, (B) quartz–organic colloid–clay domain, (C) clay domain–organic colloid–clay domain, (C_1) face–face, (C_2) edge–face, (C_3) edge–edge, and (D) clay domain edge–clay domain face

Equations 3.82 and 3.83 represent the affinity for the surface and solvent, respectively. Cations that are readily hydrated normally remain in solution, whereas large organic ions may be adsorbed at the particle–water interface because they have a low propensity for the liquid phase. This follows Traub's rule, which states that organic substances have a tendency to be adsorbed from solution based upon increasing molecular weight. Amphipathic organic molecules—those which contain a hydrophilic ionic or polar group and a hydrophobic constituent—tend to migrate to the particle surface, and also have a tendency for self-association which results from hydrophobic bonding. This self-association or micelle formation is depicted in figure 3.15.

Sorption of Contaminants

As contaminants (including pesticides, waste products, and organic chemicals) are applied or spilled onto soils, they may be preferentially adsorbed by humic substances present in the media. The longevity and hazard of the contaminant will depend on the chemicals' persistence, half-life (if applicable), leachability, volatility, degradability, and biological activity within the medium. Also, it will depend on soil parameters—such as hydraulic conductivity, infiltrability, pH, and so on. Obviously, the greater the content of humic substance present in a soil, the greater will be its capacity to buffer the deleterious effects of a contaminant. As depicted in figure 3.16, the interaction of humic substances with clay provides an organic surface for adsorption; thus, individual effects of either clay or organic matter alone are not easily ascertained. This is because the clay–humus or clay itself are the two primary surfaces that interact as an adsorbent, and because even clay particles usually have humic substances attached if any are present in the soil. In instances where herbicides are applied, the quantity of humic substances present have a large effect on adsorption (Adams and Thurman 1991; Armstrong and Konrad 1974; Stevenson 1976). Primarily, cationic organic molecules, such as those found in herbicides, are bound to the particle surface by ion exchange mechanisms (examples of these types of herbicides are diquat and paraquat). Other compounds, such as polar organic chemicals (neutral in characteristic), are bound to the surface particle primarily by organic matter, and also by clay.

The phenolic-, aliphatic-OH, COOH, enolic-, amino, and other nucleophilic reactive groups occurring in humic and fulvic acids produce chemical changes in many pesticides

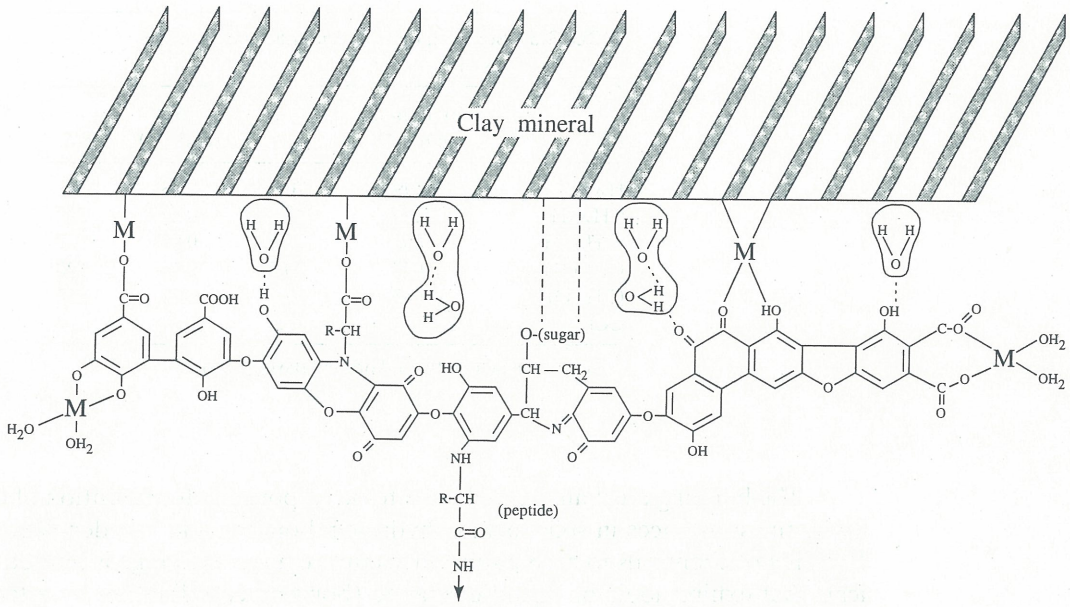

Figure 3.16 Interaction of humic substances with clay minerals; data from Mathur and Farnham (1985)

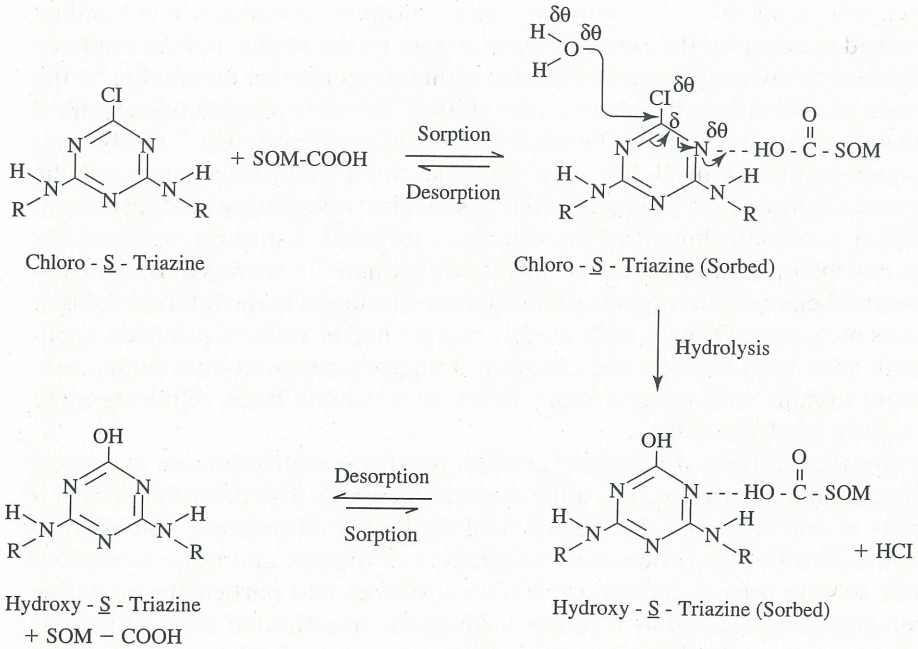

Figure 3.17 Selected reactions that take place in the hydroxylation of chloro-s-triazines

applied to soils. These chemical changes promote nonbiological degradation of many organic chemicals applied as pesticides (Armstrong and Konrad 1974). Thus, once the chemical is applied, a chemical transformation can take place. In many instances metabolites of the original chemical will be generated that may be more harmful by persisting in the soil longer than the parent compound. Reduction and hydrolysis, along with other reactions of the pesticide, can take place, all of which alter the parent. Figure 3.17 shows some of the reactions believed to take place in the hydroxylation of chloro-s-triazines.

TABLE 3.6 Sorption of Polar Liquids Compared to Dielectric Constant

Liquid	Total intake ($cm^3\ g^{-1}$)	ε	S ($cm^3\ g^{-1}$)	ε/S
H_2O	0.99	76.0	0.58	131
CH_3OH	0.66	31.9	0.25	128
C_2H_5OH	0.60	24.1	0.19	127
$C_3H_7OH_{(n)}$	0.57	20.5	0.16	128
$C_5H_{11}OH_{(n)}$	0.53	14.6	0.12	122
CCl_4	0.41	2.2	—	—

Source: Data from Winterkorn and Baver (1934).

The bonding mechanisms believed to be responsible for retention of organic chemicals by humic substances in soils include hydrogen bonding and van der Waals–London forces. Bonding of chemicals to humic substances through ion exchange is limited to organic chemicals that exhibit ionic or ligand exchange (bonding coordination by attached metal ions). Exchangeable groups may exist as cations that can become positively charged through protonation. Protonation will depend upon the pK_a of the chemical and the proton-supplying capacity of the humic substance.

Other bonding effects include the partitioning into hydrophobic media, where bonding of organics is believed to occur on the active surfaces of fats, waxes, resins, and the aliphatic side chains of humic and fulvic acids. As mentioned earlier, sometimes a metabolite to the parent may be more persistent in soils than the parent itself. This is because stable chemical linkages are formed between the organic chemical and humic substances, which tends to increase the persistence of the chemical. In fact, acylanilides and phenylcarbamates partially decompose to produce chloroamines when added to a soil. The two primary binding mechanisms appear to be a direct attachment of the chemicals to reactive sites on colloidal-size humic substances, and incorporation into newly formed humic and fulvic acids during the humification process. It is believed that organic chemicals are entrapped in the internal voids of the sievelike humus molecules. Organic soils usually require higher rates of pesticide application than mineral soils, both because the chemical is strongly retained onto humic substances and because organic soils contain more water on a volume basis, requiring more solute to obtain a given concentration.

In recent years, there has been increased concern regarding contamination of ground water by pesticides, radioactive wastes, and other organic chemicals. The primary concern is regarding transport of contaminants due to colloidal facilitated conveyance and particulate-matter transport. This transport occurs by attachment of organic and other hazardous chemicals to water soluble organic carbon (WSOC) substances and particulate matter so small that it is sometimes unstrained as it passes through the unsaturated zone, ultimately reaching ground water. Generally, WSOC concentrations are greater in the upper O and A horizons, and decrease with depth to the parent material. Concentrations of these materials are highest during spring and winter, when heavier well-structured soils are nearly water saturated and coarse-grained soils are very moist. Also, humic substances tend to increase in ground-water as the concentration of WSOC increases, primarily due to increased organic matter content within the unsaturated zone through which soil water must pass to reach ground water. Likewise, in ground waters that have a murky or colored appearance, humic substances may account for up to 65% of WSOC present, whereas in clearer water they account for only 10–30%.

Humic substances also play an important role in transport of nitrogen to groundwater (Wallis 1979). Nitrate is one of the largest non–point source pollutants in the United States; humic acids and humin contain about 2–6% N, whereas fulvic acids contain about half this amount. Except in agricultural settings and for leguminous plants, N_2 is primarily supplied to soils by the atmosphere. However, once in the soil, N_2 can be converted to organic-N. In this form, nitrogen can undergo several processes of transformation including amminization, ammonification, nitrification, and denitrification (Bremner 1967; Stevenson 1982b). During the process of amminization, organic-N is converted to various amino groups (the hydrolytic decomposition of proteins and subsequent release of amines and amino acids), which are further converted to NH_3 and NH_4^+. In the ammonium state, the N present may be immobilized within the organic matter or assimilated, or it may be nitrified to NO_3^-. The major steps of nitrogen transformation are as follows.

Microbial N-fixation	$N_2 \rightarrow$ Soil organic-N
Amminization	Soil organic-N $\rightarrow$ R-NH_2 + CO_2 + additional products + energy
Ammonification	R-NH_2 + $H_2O \rightarrow NH_3$ + R-OH + energy
Nitrification	$2NH_4^- + 3O_2 \rightarrow 2HNO_2^- + 2H_2O + 2H^+$ $2HNO_2^- + O_2 \rightarrow 2NO_3^- + 2H^+$
Denitrification	$NO_3^- \rightarrow NO_2^- \rightarrow NO \rightarrow N_2O \rightarrow N_2$

These reactions are driven by microorganisms in soils which greatly depend on temperature, pH, water content, and the amount of organic matter present. A detailed discussion of these processes can be found in Mengel and Kirkby (1982). For further understanding of nitrogen and its role in soils, the reader is referred to Stevenson (1982b).

3.9 AGGREGATION

Sections 3.9 through 3.12 discuss aggregation, aggregrate formation, crusting, and cracking of soils. To understand each of these sections, it is important to understand the primary causes of separation, chemical bonding, hydration, swelling, slaking, flocculation, and dispersion of clay–water interactions that were discussed previously.

In chapter two, we discussed the three separate phases of a soil (solid, water, and air) and how these phases combine to form the soil matrix. Further discussion revealed that the individual particles combine to make up the soil structure (the arrangement of soil particles). Individual, primary particles of sand, silt, and clay combine by biological, chemical, and physical means to form secondary particles or aggregates. From chapter 2, the reader may recall that aggregates can be defined as a group of two or more primary particles that form a cohesive mass stronger than the surrounding soil mass. Natural aggregates that vary in their water stability are called *peds* (also known as macroaggregates), whereas the term *clod* refers to a soil mass broken into various shapes by artificial means such as earthmoving activities or tillage. Soil peds broken into pieces are termed *fragments*. *Concretion* refers to a coherent mass formed within the soil by chemical precipitation from percolating ground water.

As with soil profile formation, the formation of aggregates is directly affected by the parent material, climate, and presence of vegetation. Generally, the more vegetation, the greater the organic complexing and cementation there will be for aggregate formation, due to biological activity. Many soil properties, including water retention capacity, infiltration, and transport, are directly dependent on the amount of aggregation present. In figure 3.18,

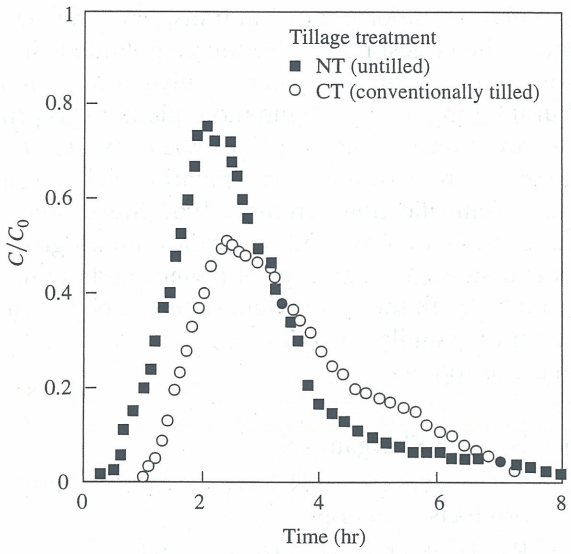

Figure 3.18 Example of a conservative tracer (potassium bromide) pulse (BTC) through aggregated, untilled (NT), and conventionally tilled (CT) Cecil series soils (Georgia, U.S.A.). C is measured and C_0 is initial concentration

chloride movement through a highly aggregated, untilled soil is compared to that through a conventional tilled, little-aggregated soil. Water movement is faster in the untilled soil, due primarily to its greater aggregate content.

The USDA has described and classified soil aggregates based upon their size, shape, and edge–face characteristics. They use three main categories for description: class or size of structure, type or shape of structure, and the grade of the structure and its durability. There are four (as illustrated in figure 2.4): **(1) Blocky**—vertical and horizontal cracking are equally developed, giving peds approximately equal axes. The tops, which may be flat or rounded, fix together upon swelling so as to leave no space or gaps between contiguous peds. **(2) Spheroidal**—these differ from the blocky type in that they are rounded, and when they are wet leave a fairly uniform distribution of pores between contiguous peds. **(3) Laminar**—natural cracking is generally horizontal. **(4) Prismatic**—vertical cracking is often exhibited, with the ped faces appearing relatively smooth and flat. These grades can be further divided into subgroups for more exact classification.

One of the most important criteria for soil classification is the grade of structure, which depends on the durability of aggregates and the proportion of aggregated and nonaggregated soil particles. There are four grades of structure: **(1) Structureless**—no observable aggregation; **(2) Weak**—weakly formed individual peds that are barely discernible in undisturbed soil; **(3) Moderate**—well-formed, distinct peds that are moderately durable but not distinct in undisturbed soil; and **(4) Strong**—durable peds that adhere weakly to each other and are readily evident in undisturbed soil.

As with the classification of types of structure, the various structural units within the soil can be classed into four separate size groups: **(1) Domains**—groups of clay particles ranging in size to about 5 μm, consisting of inner pore concentrations of approximately 20 nm and interdomain pores of about 100 nm; **(2) Granules**—groups of domains, fine sand, and silt particles cemented together, ranging in size to about 0.5 mm; the larger particles do not break apart on wetting (this group is also known as microaggregates or microcrumbs); **(3) Crumbs**—groups of granules ranging in size up to several millimeters; and **(4) Clods**—aggregates $>$ 1 cm that, when broken apart, form crumbs.

The presence of aggregates within the soil is one of the factors affecting the nature of soils. Buildings, roads, bridges, other types of construction, tillage operations, plant growth,

and soil mechanical properties are all influenced by soil structure. The growth of plants can be promoted by the presence of aggregates, which form natural cracks for root penetration to greater depths within the soil profile. Water also moves to greater depths, due to the presence of these cracks. Chemicals in this water contact fewer adsorption sites and, thus, have a greater potential for contaminating groundwater. Soil compaction is difficult in the presence of large aggregates, complicating the erection of large structures. Soils with little structure and aggregation confine the movement of water, restrict plant growth, and make drainage difficult.

QUESTION 3.15

Figure 3.18 shows a comparison of breakthrough curves (BTC) for a conventional tilled agricultural soil versus an untilled soil. Much of the literature on solute transport also deals with BTCs. What is the importance of a BTC; that is, why are they useful?

3.10 AGGREGATE FORMATION AND CHARACTERIZATION

Aggregation begins with the binding together of colloidal particles in the form of loose and irregular floccules, due to the presence of the electrical double layer. The collision of particles results in a mutual attraction when the electrokinetic potential is sufficiently low; consequently, a floccule is formed. Through chemical and biological activity, these floccules combine together to form aggregates.

Aggregation is primarily influenced by the amount of clay present. The flocculation of the clay, plus cementation by chemical and especially biological activity within the soil, is what forms aggregates. Clay flocculation does not form a stable aggregate because the clay is usually not strong enough to bind aggregates together into stable masses. However, the addition of cementation by root exudates and biological activity can form very stable aggregates. These cementing agents are usually sesquioxides, organic matter, humus (by adsorption of cations), silicate clays, lime, and polysaccharide gums (Wild 1988).

The expansion and shrinkage of soil upon wetting and drying, freezing and thawing, faunal activity, water movement, and root activity are the primary factors involved in aggregation. These factors vary greatly, dependent on climate and geographical location as discussed in chapter 2. Three primary mechanisms are responsible for aggregate formation: biological, chemical, and physical. Figure 3.15 represents the suggested arrangement of the various particles which compose soil aggregates. Quartz crystals are bound by several types of associations: (A) quartz–organic colloid–quartz, (B) quartz–organic colloid–clay domain, (C) clay domain–organic colloid–clay domain, (C_1) face–face, (C_2) edge–face, (C_3) edge–edge, and (D) clay domain edge–clay domain face (Emerson 1959).

Biological

The biological mechanism of aggregate formation is composed of both plant and animal activity, usually in the form of microbial decomposition and degradation of organic matter, and the decay of dead fauna. As organic matter is added to the soil, the microbial population flourishes, producing intense activity which helps decompose the organic matter. The primary microbial participants are actinomycetes, bacteria, fungi, algae, and protozoa. As the organic matter is decomposed, it is synthesized into various forms of organic material. Both actinomycetes and fungi produce branching and individual filaments termed conidia and mycelia, respectively, which help bind the synthesized organic material together.

While the actinomycetes and fungi are primarily responsible for mechanical binding of soil particles, bacteria, roots, and fauna such as earthworms create polysaccharide gums, casts, and other cementing agents that further bind the organic materials. These functions are dependent upon favorable climate and upon the species of organism present, itself a function of an available energy source and soil nutrients (such as nitrogen) that aid in the decomposition process. A comparison of temperate and tropical region soils to arid zone soils indicates that soils high in organic matter form more water-stable aggregates than soils in arid zones, which are low in organic matter and are sparsely aggregated.

The effects of plant and root growth and distribution affect aggregation. The plant canopy shields the soil surface directly beneath it from mechanical energies originating from raindrop impact, preventing aggregate breakdown and dispersion (physical). Plant root systems, especially those of annuals, continually rejuvenate themselves during early and mid-growth stages. As a result, old roots die, while new roots form to obtain water and nutrients for the plant. This has a dual effect. As the old roots die, they decompose and become food for the microbial population of the soil, which synthesizes them into organic complexes (biological). The new roots excrete polysaccharide and polyuronide gums from epidermal and cortical cells, which serve as additional binding agents for the surrounding soil (chemical). This assists in the formation of microaggregates which can later form macroaggregates. Additionally, roots create channels and large pores as they penetrate the soil, allowing more water and air movement. This increases water and nutrient supply, and biological activity, to greater depths in the soil profile (physical).

Large areas covered in grass such as pastures, sod farms, and golf courses have extensive root system development and usually promote the formation of very stable aggregates, due to the physical action of the roots on the soil and chemical and biological effects. As a result, root exudates and microbial decomposition are responsible for binding together small aggregates into large stable aggregates. In special agronomic circumstances such as rice production, aggregates are destroyed in the process of puddling the soil to prevent or greatly retard water loss due to infiltration. However, the oxidizing ability of roots on iron and other reduced matter, along with root exudates, regenerate aggregates.

Chemical

The formation of aggregates through chemical means is achieved by ionic and hydrogen bonding between carbonyl groups and oxygen atoms within the layered clays. The ionic bonding is accomplished through cation bridging, which bonds the organic complexes to the clay surface. Additional bonding mechanisms are van der Waal's forces and sesquioxide–humus complexes. It is commonly known that calcium tends to flocculate a soil, whereas oversaturation with sodium will disperse the soil and break apart aggregates. Calcium and other divalent cations (such as magnesium) will bind the granules together by acting as a cation bridge between the clay and organic colloids as follows: Clay-Ca^{2+}-OOC-R-COO-Ca^{2+}-Clay. Aggregate formation in this instance depends on the interaction between the exchangeable cations held by the clay particles and soil pore water. Because of the presence of the electrical double layer, the negatively charged clays are surrounded by both fixed and mobile cations, causing water dipole orientation along the lines of force in each ion's electrical force field and the force field of the negatively charged clay. This causes the formation of cation–dipole linkages between separate clay particles. As dehydration occurs around the particles, the ions share water envelopes that form a calcium or magnesium linkage between clay particles, resulting in the formation of stable aggregates. Similar circumstances can occur with polyvalent cations.

Other organic substances, such as humic acids will not attach directly to clay surfaces because of their negatively charged surfaces, they form complexes with soluble sesquioxides that have been deposited on the surfaces of clays (Dawson et al. 1981). Humic acids can also be coordinated with Al^{3+}, Ca^{2+}, Fe^{3+}, and Mg^{2+}, which act as cation bridges between the clay surface and humic acid. Soil aggregates are divided into two groups, based upon their association with divalent or trivalent ions. When associated with divalent ions, the clay–organic complexes are saturated with calcium and magnesium, forming microaggregates. When associated with trivalent ions, soluble sesquioxides are deposited on clays forming complexes with humus, also forming microaggregates. It is the latter group that forms stable soil aggregates.

Additional chemical factors that influence soil aggregation are hydrogen bonding and cation exchange. As mentioned at the beginning of this section, hydrogen bonding can occur between carbonyl groups (on organic molecules or complexes) and the oxygen atoms of the clay crystal. When the charge on organic matter is not satisfied, ionic bonding with hydrogen is very strong, much the same as when polysaccharides with carboxyl groups attached are adsorbed to the clay surface. Due to the nature of charge in soils, the system favors adsorption with complexes and materials not conveying a charge. This could be the effect of van der Waal's forces, which become stronger as dehydration of the soil occurs. The effects of cation exchange can either flocculate or disperse a system, a good example being calcium and sodium. Calcium is known to flocculate soils as (illustrated by the application of gypsum to agricultural fields). In contrast, sodium-saturated soils are more hydrated and dispersed than calcium-saturated soils. This is not true for acid soils where hydrogen is the dominant cation, although other cations may be present in abundant number (such as aluminum and iron); particularly if the soil is of the sesquioxide type. In acid soils, the adsorption of calcium is associated with the organic colloid fraction, because H^+ saturated soils are usually not well flocculated.

Physical

Various aspects of the physical phenomena which cause aggregation have been discussed. These include freezing and thawing, shrinking and swelling, and the effects associated with colloidal clays. Reflecting on the discussion in chapter two about soil formation, we remember that wetting, drying, swelling, and shrinking, which are somewhat interdependent, occur in alternate cycles. As the soil wets and subsequently dries, the soil mass is separated or broken into smaller fragments due to shrinking. Depending on the soil type (whether it be a 1:1 or 2:1 clay), the water content of the soil can have significant effects on aggregate formation. This causes the shape and formation of various types of structural peds. These properties are responsible for slaking (the destruction of aggregates upon wetting), mudslides, and other soil events.

The loss of water from a soil as it dries allows air to enter pores, increasing the total volume of air present while decreasing the amount of water. This decrease of soil volume upon drying is due to both the loss of water and the cementation of soil particles because of a collapse of pore size. The solid soil mass does not change. This means that soil shrinkage is less than the volume of water lost due to evapotranspiration and plant use. However, as the soil rewets, the volume will be greater, because air is occluded in various pores, and because of swelling.

Slaking occurs when a dry soil is rewetted. Rewetting of a dry soil has two effects: occluded air within the soil pores is compressed, which causes minute explosions within the pores, disrupting the clod (this is the major cause of slaking); and absorption of water causes

unequal swelling within an aggregate, resulting in fractures along the cleavage planes. The rewetting of a dry soil also involves two forces, namely matric and cohesive. As the soil first begins to wet, matric forces exceed cohesive forces but, as the soil becomes more saturated, destruction of the cementing bonds between particles occurs, causing a loss of cohesion and breakdown of the aggregate.

An example of some of these processes may be found in the instance of mudslides. Mudslides usually occur when a soil has an overlying layer of organic material or loose alluvium from deposition due to erosion, landslides, or winds. The slide will usually occur under a heavy rainfall event. The overlying alluvial soil layer becomes rapidly saturated as the wetting front moves vertically through the soil. This drives soil air ahead of the wetting front, entrapping it between the upper alluvial layer and the second layer of soil. (Air can only be trapped to a pressure equal to the air entry pressure of the soil. At greater pressures, the air will quickly escape, being more than fifty times more mobile than water). Additionally, compression of occluded air causes slaking of aggregates that may be present in the alluvial layer, with an overall loss of slope stability that is also promoted by the loss of cohesive forces as the soil saturates. The upper layer becomes very heavy due to the additional weight of water absorbed and begins to slide: the development of the entrapped air layer maintains dry conditions at the interface of the second soil layer and, of a sudden, the entire slope moves. In mudslides, slaking would be of minor importance; the major factors are entrapped air and loss of cohesive forces. Thus, the breakdown of soil aggregates and instability of soils can be attributed to reduction in cohesive forces, destruction of cementing bonds, entrapped air, and the stress–strain relation in alternate wetting and drying cycles. Erosion is also a major factor, causing slope instability and aggregate breakdown (Davies and Payne 1988).

Freezing and thawing of soils can both form stable aggregates and destroy soil structure. When a soil cools slowly, a smaller number of large ice crystals are formed. These crystals partially melt during the thawing cycle; the remaining crystals serve as a foundation for further freezing. As these crystals form, water is drawn to them during the freezing process, which dehydrates the surrounding soil. The crystals expand in the process, compressing the dry soil in the immediate vicinity. The combination of both these parameters causes aggregation. However, if the soil is frozen rapidly, the formation of a large number of crystals can cause aggregate destruction. When performing laboratory analysis on intact soil columns, care should be taken not to freeze them, as this will cause a breakdown of soil structure not visible to the naked eye and also develop artificial gradients within the soil by dehydrating the soil around larger ice crystals that may form. This consideration can be critical in contaminant transport studies, possibly biasing results.

QUESTION 3.16

We have discussed how aggregates can be broken or dispersed and pores compressed or destroyed by earthmoving and agricultural activities. What environmental forces can cause the same results?

3.11 SOIL CRUSTING

Under conditions of heavy rainfall and irrigation, crust formation on soil surfaces is due to soil aggregates breaking apart because of the kinetic energy of raindrops that may cause compaction in the upper surface layer, and clay and its cementing agents possibly being dispersed from quartz crystals that clog the overlying surface pores due to physiochemical dis-

persive effects. The larger the raindrop, the more kinetic energy it possesses and the greater the aggregate breakdown and dispersion; thus, larger drops will destroy the original structure to a greater depth (Miller and Radcliffe 1992). Crusts under these conditions may be 5 mm thick. As the aggregates break apart, the finer clay particles slowly wash into the soil pores, reducing infiltration and causing erosion on sloping soils. Generally, the greater the clay content and the heavier the rainfall, the thicker will be the soil crust that forms. As the soil dries, the top layer, which is now composed of very fine clay and silt particles, shrinks. Depending on the major ions present in the soil, the edges of the crust will crack and sometimes curl. If the soil is inhomogeneous parallel to the surface, curling or peeling will occur; inhomogeneity normal to the surface will cause cracking (both occur during the drying stage). In arid regions, the predominant ion is sodium, which causes dispersion and tends to form thin crusts that curl upward at the edges. In more temperate regions (such as the southeastern United States), where aluminum and iron sesquioxides abound, crusts tend to be very hard and thick with little edge curling.

Close examination of a soil crust will reveal what soil scientists call depositional crusting, where an actual structure has developed during crust formation. Normally, a stratification is present in which the larger particles are deposited first, followed by successively finer particles, with the very finest particles deposited at the top of the crust. These form an effective seal or barrier. The crust reduces infiltration while also reducing evaporation and, as mentioned earlier, can be a significant factor in causing erosion. The soil crust is marked by a high bulk density, due to the presence of quartz crystals in the underlying layer of the crust. As the crust dries, the cementing agents present at the initial dispersion of the aggregate enhance cementation of the particles, causing a very hard crust. Most soil crusts are thin (< 2 mm). Typically, a soil crust may be characterized as possessing stratification, high bulk density (compared to surrounding soil), and a low non-capillary pore space. Once dry, the crust is harder than the remaining soil mass, due to particle cementation. Environmentally, soil crusting encourages run-off and erosion which, when contaminants (such as agricultural herbicides, fertilizers, and industrial and municipal wastes) are present, can pose hazardous conditions for both surface and groundwater pollution. Factors commonly associated with soil crusting are high ESP, high silt content, and low organic matter content. Soils that have high organic matter content, and those that are mulched by straw or artificial barriers (such as plastic mesh), have a low susceptibility to crusting.

Soil texture, steepness of slope, and aggregate stability are three of the major physical factors that greatly affect crusting potential. A crust can form on almost all soil textures; textures most likely to form crusts are those with high silt contents. Also, crust formation is more likely to occur on sandy loams than on clay loams. Textures that are unlikely to form crusts are those with low clay, silt, and coarse sand contents. The steepness of slope is usually inversely proportional to surface sealing or crusting, due to several factors. As slope increases: there is usually a decrease in the number of raindrops per unit surface area and, thus, a subsequent decrease in total kinetic energy; interrill erosion also increases, which erodes a large portion of formed crusts; and rill density and depth increase, which increases surface roughness, making formation of crusts less likely. If the slope is resistant to crusting due to textural properties, these factors would not affect sealing or infiltration. Consequently, the general characteristic of slope steepness on crusting is that as slope increases, soil strength decreases, which results in an increase in infiltration. Generally, as aggregate stability decreases, the potential for crust formation increases. Also, if aggregates are large, a longer period of time is required for crust formation than with small aggregates. Additionally, the water content of the aggregate at the time a rainfall event occurs can dramatically affect crusting potential. Normally, initially dry aggregates deteriorate from rainfall effects due to slaking. Such aggregate breakdown causes a rapid filling of interaggregate spaces with smaller aggregates,

which break down very rapidly to form a crust after drying. However, if the aggregates have a high water content during rainfall, the slaking process is unlikely to affect their breakdown, and the intensity, duration, and related energy of raindrop impact will be the primary factor affecting aggregate deterioration. Under these conditions, there is a low potential for crust formation. Also, the rougher the soil surface, the less likely a crust will form, despite silt content, unless the aggregates and soil surface are very dry and the initial rainfall event is very intense and of a duration of longer than about forty minutes.

There are two major categories of crusting, structural and sedimentary (Sumner and Stewart 1992). *Structural crusts* are generally formed in response to the direct physical reactions and processes associated with raindrop impact. A soil with a high clay content (20–30%) and the presence of stable aggregates can have several layers within a crust. Each layer is formed by rainfall-induced aggregate breakdown, soil particle or aggregate rearrangement, and the coalescence of aggregates. The entire crust may be relatively thick (1 to > 10 mm). A thin layer or microlayer may be formed at the surface due to aggregate breakdown and deposition from suspension at the end of a rainfall event. This is termed a skin seal, which is more typical in readily dispersible soils and soils high in sodium content. Another microlayer may be what is termed a washed-out layer, which is formed from disjunction of clay particles from quartz crystals. Essentially, the clay is mechanically removed from the soil particle by rainfall, and then the surface of the soil is sealed. This type of action is readily seen on piedmont soils in the southeastern United States. After a heavy rainfall event, individual quartz crystals from which the clay has been removed are readily visible. Occasionally, the micromass removed from the surface particles may form a micromass-enriched layer by translocation of the mass a short distance below the surface. This type of crust is termed a washed-in layer. Also, aggregate coalescence can form a disruptional layer. All of these microlayer crusts can be formed during a rainfall event within one soil. However, it is unlikely that all of these microlayers would be found in a single structural crust.

The skin seal is primarily a dense layer (0.002 to < 0.1 mm) of fine particles at the surface of a structural crust. The most likely mechanism for formation of a skin seal is the deposition of clay particles from suspension at the end of the rainfall event. The basic evidence proposed for this is the occurrence of the skin seal over washed-out layers, and the uniform orientation of the clay particles within the skin seal. Also, it is likely that continual raindrop impact on such a thin layer would destroy it; thus, it is indeed likely that these seals do not form until the end of a rainfall event. Washed-out layers (< 1 mm) occur at the surface or lie under a skin seal and appear as skeletal grains with no associated clay or micromass. If a washed-in layer is present, it will be subjacent to the washed-out layer and generally < 1 mm thick. If runoff is a problem on particular soils, the clay materials stripped from the skeletal grains may move laterally with the runoff and, thus, cause an absence of a washed-in layer. Typically, increases in ESP values from low to high (2–10) can substantially contribute to the formation of washed-out and washed-in layers. Electrolyte concentration and composition in rainwater and clay mineralogy will affect soil dispersibility. The disruptional layer is a function of initial aggregate size. If the media surface is initially dry, the rapid wetting of the aggregates will cause slaking, resulting in swift aggregate breakdown. Also, as aggregates become wetter, aggregate strength is reduced to a point at which the stress imposed by raindrops disrupts the aggregate. At this point, the disruptional layer forms rapidly, releasing particles from individual aggregates into interstitial spaces between aggregates, creating a smooth layer with reduced porosity. As much as a 90% reduction in porosity may result due to structural crust formation.

Sedimentary crusts generally result from the transport of particles from relatively higher to lower topographic locations or positions. This transport is normally induced by runoff, and may cover long distances. Sedimentary crusts are sometimes referred to as depositional

crusts. As one would suspect, when the flow velocity slows, larger particles are deposited first, followed by finer particles. This is normally the result of decreasing slope and/or reduced rainfall volume. In fact, for sedimentary crusts to form, the rainfall rate must be greater than the infiltration rate, and the capacity of the runoff to transport must be less than that required to completely remove the individual particles from the site. Sedimentary crusts range in thickness from 0.6–20 mm, and may reduce porosity by as much as 91 percent. A common feature of such crusts are circular voids (vesicles) found directly below the soil surface, which appear to be due to air entrapment because of ponded water during intense rainfall events (West, Chiang, and Norton 1992).

There are a number of cementing agents that are related to aggregation of soil and its structural stability. These include silica, organic materials, iron and aluminum sesquioxides, cations, and other cementing agents. The effectiveness of a cementing agent depends upon its solubility, and whether the solid phase is in equilibrium with the dissolved phase (or dries irreversibly, or rehydrates and redissolves on rewetting). Additional factors include, whether the dissolved phase ionizes, remains as an undissociated molecule, or precipitates as discrete particles or surface coating (such as sesquioxides); and whether it is crystalline or noncrystalline, or can acquire a charge.

The most common cementing agents in arid and semiarid regions are silica, gypsum, and lime. In the humid tropics, noncrystalline hydrated aluminosilicates and sesquioxides are the most likely cementing agents. For cementing action to occur, one soil particle must be brought into close proximity with another. This will depend on the number of particles per unit volume, which depends on soil texture, particle shape, and packing (as discussed in chapter 2). Both the soil water and solutes will determine the spatial arrangement of the soil particles within a crust. Consequently, a nearly saturated or saturated condition is necessary at the surface for a crust to form. Soil water tension increases as the soil dries, bringing soil particles closer together, and soil pore sizes decrease due to clogging. The combined effects of these basic processes stimulate bond formation, thus inducing crust formation. The reverse is also true: as water is added to most crusts, they lose their strength as a result of swelling and softening of cementing agents. Soil inhomogeneities attributed to uneven packing and flocculation influence the stress distribution in a drying soil, which also determines crust characteristics. In lateritic soils, extreme desiccation causes irreversible hardening and crusting. Additionally, although organic matter usually aids in preventing crust formation, it is the overall mixture of organic matter prior to drying that has the greatest influence on soil surface conditions after drying.

One other crust type that deserves mention is prevalent in the western United States and other arid regions throughout the world. This is a chemical crust that is essentially a salt incrustation or deposit on the surface, caused by evaporation. The most common forms are sodium chloride, carbonate, and sodium sulfate chemical crusts. Other minerals, such as bloedite, gypsum, epsomite, and hexahydrite, can also be found in these chemical or evaporative crusts—depending on geographic region and soil type (Timpson et al. 1986).

There are two common methods for measuring crust strength: modulus of rupture, and balloon pressure. The modulus of rupture measures the breaking strength of a crust, and is the maximum stress that a crust will withstand without breaking. Generally, a soil sample is subjected to a bending force. The specific surface area, mechanical composition, and ESP appear to be linearly related to the force required to rupture a specific soil sample. However, there is also an inverse relation between the modulus of rupture and particle size distribution. The modulus of rupture is given by

$$\sigma_r = \frac{3F_b L}{2bd^2} \tag{3.84}$$

where σ_r = modulus of rupture (dynes cm^{-2}), F_b = breaking force applied at the center of the soil sample beam span (dynes), L = distance between the sample and support (cm), b = width of sample (cm), and d = sample thickness (cm). It has been established that the modulus of rupture is strongly correlated with hydrous mica content of soil.

Crust strength is also measured by balloon pressure. A balloon is buried in the soil, and the pressure required to inflate the balloon to the point where the crust begins to crack is determined. Cone penetrometers are also used to measure crust resistance or strength. It should be recognized, however, that the various methods of crust strength measurement were originally designed for agricultural purposes. The primary purpose was to imitate the process by which seedlings force themselves upwards through a crust, to determine the minimum strength that would inhibit germination. Environmentally, strength tests are valid for determining possible rates and time of runoff due to rate of crust formation for given soils.

Generally, crust strength is higher in natural soils that have a high silt and fine sand content. These types of soils are structurally unstable when wet. In arid areas where sodic soils predominate, osmotic swelling forces attract water into the diffuse electrical double layer. This causes dispersion, which separates individual clay particles by breaking particle-to-particle bonds. As a result, sodic clays are drawn into a closely oriented, laminated configuration by surface tension during drying. As the surface area increases for certain clay minerals, more stress occurs on the crust during drying; consequently, more fracture planes develop. As a rule of thumb, crust strength will increase by about a factor of three as water potential at the surface decreases from −33 kPa to −1500 kPa. Normally, the process of wetting removes soil air; when this happens, crust strength can significantly increase. Thus, flooding can significantly increase crust strength and cementation properties.

There are environmental hazards associated with crust formation. As crusts form, the hydraulic conductivity of the soil is greatly reduced because of the impermeable crust now overlying it. This will cause increased runoff and possible herbicide contamination of nearby surface waters in industrial and agricultural areas. Erosion also becomes a severe problem in some soils, which can result in the deterioration of surface water quality due to silt and clay content. This can decrease oxygen supplies in the water, causing high death rates of aquatic species. In an environmental setting, the soil acts as a natural filter for chemicals which adsorb, exchange, degrade, and so on, as they pass through the soil matrix. The formation of a crust usually impedes the penetration of these chemicals through the soil and they are subsequently transported by runoff processes.

3.12 SOIL CRACKING

Various soil types are prone to cracking upon loss of water. Vertisols and alfisols both exhibit a high degree of shrinking and swelling; consequently, cracks develop that can expose additional surface area for water loss due to evaporation, accelerating the drying process. These two soil types are characteristically dark, having uniform fine or very fine texture and a low content of organic matter; but perhaps their most important property is the dominance in the clay fraction of expanding lattice clay, usually montmorillonite, that causes large volume changes with small changes in water content. The area where the soil cracks is termed a cleavage plane. Typically, as shrinkage progresses, cleavage planes develop at the points of least resistance, which correspond to the plane of highest water content. Cleavage planes develop both vertically and horizontally, producing irregularly shaped cracks that may be > 1 cm wide and > 50 cm deep (Sumner and Stewart 1992). Such cracks can facilitate the penetration of water and associated contaminants during periods of heavy recharge, inducing a high risk of contamination of groundwater.

The development of cracks can drastically change the hydrology of a given soil and, due to the presence of high clay content (> 30%), the water content in the soil may vary from complete saturation to less than the wilting point. With the onset of the dry season, the soil dries, shrinks, and cracks to form large prisms. Further drying takes place from the crack surface; if there are soluble salts or inorganic contaminants present, they may form an efflorescence on the surface of each prism. With the first significant recharge event, water flows rapidly down the cracks along the surface of the prism, dissolving salts and flushing other chemicals out of the soil, leaching these chemicals deeper into the profile. Frequently, the water table may be within 1.5 m of the surface, which can cause quick contamination; often, the entire soil profile becomes saturated with water until surface ponding occurs.

Normally, the crack pattern developed on the surface of a uniform, drying soil will appear as a group of polygons, essentially similar in both size and shape. This is especially true when the pattern is constricted by the use of devices such as ring infiltrometers or barrels filled with soil for testing. However, under ideal conditions, the polygons will be hexagonal in shape, with the cracks meeting at a 120° angle. Generally, subsequent cracks occur at right angles to existing cracks. As each new crack is formed, the cleavage plane from which it departs allows the release of strained energy only on the side on which the new crack is located. Consequently, new cracks will not normally cross existing cracks. These characteristics are true only for bare soils. On soils that have cultivated crops, cracks will tend to form parallel to the plant rows—both between and around the plants, and within the furrows. In the presence of sporadically placed trees, plants, and grasses, irregular polygonal patterns also tend to form. Major crack formation will tend to form not directly around the plant or its roots but away from the plant in bare soil. This is probably the result of the physical and biological effects of root systems responsible for stable granulation. It is well known that roots secrete organic cementing substances for aggregate formation; this would probably reduce the tendency for crack formation directly around the root.

Cracking takes place when the release of energy per unit area of the crack is greater than the increase of surface energy. There are two separate energy terms, and the balance between them determines the amount of cracking that will occur. These terms are free surface energy due to new surface exposure, and energy released per unit free surface. Free surface energy due to new surface exposure is described mathematically as

$$\frac{d\mu}{dA} = 2\gamma_m \tag{3.85}$$

where μ = energy of medium under consideration, A = area due to new surface exposure by cracking, and γ_m = surface tension or energy of the material. Energy released per unit free surface is described by

$$\frac{d\mu}{dA} = \frac{\tau\sigma_s^2 D}{E} \tag{3.86}$$

where τ = tensile stress normal to the plane of the crack, σ_s = limiting stress (dyne cm^{-2}), D = major diameter of the crack (which is assumed to be elliptical), and E = Young's modulus of the material. A combination of equations 3.85 and 3.86 yields the well-known Griffith theory for crack propagation, as

$$\sigma_s = \sqrt{\frac{2E\gamma_m}{\pi D}} \tag{3.87}$$

where the equation has been modified to make it applicable to plastic materials such as soils, which exhibit a measurable deformation before rupture. Deformation in porous media

begins when the limiting stress (σ_s) is applied. When $\sigma = \sigma_s$, the critical strain-energy released rate (G), is given as the relation,

$$G = \frac{\pi \sigma_s^2 D}{E} \tag{3.88}$$

Both σ_s (determined from the modulus of rupture) and E depend on θ_{soil} and ${}^b\rho_w$. D can be estimated from pore size distribution or particle size analysis. Thus, G/D (dyne cm^{-2}) is the energy released per unit area per unit length of crack, and can be used to characterize soil cracking behavior. The value for Young's modulus (E) has normally been obtained from the measurement of pulse transmission velocity using ultrasonic assembly, in which E is expressed as

$$E = \rho_b v^2 \tag{3.89}$$

where ρ_b = wet bulk density (g cm^{-3}) and v = pulse transmission velocity. Assuming that both σ_s and E are known, the occurrence of cracking as a function of soil water content can be predicted by

$$\sigma(\theta) < \sqrt{\frac{\frac{G}{D}(\theta) E(\theta)}{\pi}} \tag{3.90}$$

where a value of $\sigma(\theta)$ that satisfies the inequality represents a condition in which no cracking can be expected, and where the notation (θ) represents the dependence of the quantity on water content (i.e., E(θ) is read, "E as a function of θ").

QUESTION 3.17

Give several examples of processes in which flocculation and dispersion of clay is important.

SUMMARY

Flocculation and dispersion play an important role in the physical and chemical behavior of soil colloidal fractions, particularly in the areas of colloidal facilitated transport, crusting, infiltration, cracking, and swelling, as related to unsaturated zone investigations.

In this chapter, we discussed van der Waals–London forces and how they can be thought of as short-range, electrostatic attractive forces. The interaction between uncharged soil particles and water, the surface charge of clay minerals, and ion distribution and exchange were also discussed, including how these parameters affect clay–water behavior. This led to a discussion of the double layer theory, including zeta potential and the four types of electrokinetic effects normally observed in association with the double layer (streaming potential, electroosmosis, eletrophoresis, and the Dorn effect). Following a discussion of electrokinetic properties of clays, we presented the reversible process of ion exchange, which is the ability of cations and anions to exchange between the solid and liquid surfaces in a system. This was followed by a discussion of the sodium adsorption ratio of soils, an important characteristic in arid areas such as the western United States, Egypt, Israel, Nigeria, Iran, and Iraq. We also discussed the evolution of heat from a dry particle when immersed in water, termed the heat of wetting, and how it is induced by the electric field surrounding clay particles, because of a decrease of internal energy of the water molecules within the field.

The DLVO theory, hydration and swelling, and flocculation and dispersion of clays were presented in a quantitative and practical-application fashion for a clearer understanding of the forces of attraction and repulsion associated with clay–water systems. Subsequent sections discussed the importance of humus in soils, followed by aggregate formation and the physical, biological, and chemical principles responsible for that formation. The chapter concluded with discussions of crusting and cracking, which relate directly to flocculation and dispersion in soils. Throughout, it has been apparent that both dispersion and flocculation are governed by the attractive and repulsive forces associated with the electrical double layer, and by reactions between adjoining double layers as presented in the DLVO theory. The double layer is essentially composed of a charged clay-particle surface, typically termed a colloid, plus the diffuse cloud of counterions that serve to neutralize that colloidal surface.

ANSWERS TO QUESTIONS

3.1. Assuming a dielectric constant, D, of 80 and a permittivity of 78.8 esu^2/erg · cm, equation 3.12 may be used to determine the heat of hydration of this ion, such that $W = -$ [[(1)(4.803 × 10^{-10} esu/ion]^2/[(2)[(1.33 + 0.7) × 10^{-8} cm/ion]] * [(6.02 × 10^{23} ion/mol)] * [(80 − 1)/(78.8 esu^2/erg · cm)] = −3.43 × 10^{12} erg/mol. Note: e = 4.803 × 10^{-10} may be used here for other unit systems, because it readily converts to erg/mol by multiplying by 2.389 × 10^{-8} cal/erg to obtain kcal/mol. Also, regarding the negative sign, the electric force of the charged sphere on the unit positive charge (i.e., the field) acts in a direction opposite to that in which the charge is being moved. Because both the field and the direction of transport are vectors (quantities with both direction and magnitude), and because the vectors point in opposite directions, their product is negative. For example, the product of two vectors A and B is AB cos θ, where θ is the angle between the two vectors. If the vectors are in opposite directions, θ = π and cos θ = −1 and the product is $-AB$. Additionally, Voet's equation (3.12) is considered more appropriate for ions belonging to alkaline metals, alkaline earth metals, and trivalent closed-shell ions. Voet's equation can be converted to Born's equation by replacing (r + 0.7) with r in the denominator of the left-hand side for use with other ions.

3.2. Because of the units of e, k = 1.381 × 10^{-16} erg ion^{-1} K^{-1} = 4.139 × 10^{-11} mV esu ion^{-1} K. Thus, $C = C_0$ exp − [(1)(4.803 × 10^{-10} esu ion^{-1})(−100 mV)/4.139 × 10^{-11} mV esu ion^{-1} K^{-1}) × (298 K)] = −3.8925. Hence, C = 2.5 × 10^{-2} M exp(3.8925) = 1.22 M. If units for e are coulombs, then e = 1.6021 × 10^{-19} coulombs, and at 25 °C, kT/e = 25.69 mV; thus, e/kT = 38.925 V^{-1}. The answer is the same; however, the student may wish to check the problem using the other units (remember to convert ψ to potential in these units, rather than mV as in the preceding answer).

3.3. First, n must be converted. This can be accomplished by multiplying by Avogadro's number (N_A). Thus, 3.1 × 10^{-2} mole L^{-1}(N_A) = 1.867 × 10^{19} ions cm^{-3}. Hence, σ = [(2)(78.3)(1.867 × 10^{19} ions cm^{-3})(1.381 × 10^{-16} esu^2 ion^{-1} cm^{-1} K^{-1})/(3.1417)] sinh[(1)(4.803 × 10^{-10} esu^2 ion^{-1}) (75 mV)/(2)(4.139 × 10^{-11} esu mV ion^{-1} K^{-1})(298 K)]. Thus σ = (6.19 × 10^3 esu cm^{-2}) × sinh(1.4603) = 1.261 × 10^4 esu cm^{-2} or 2.626 × 10^{16} meq cm^{-2}. This problem can also be calculated by assuming that kT/e = 25.69 mV at 25 °C, so that e/kT = 38.925 V^{-1} and k = 1.381 × 10^{-16} erg K^{-1} ion^{-1}, which is converted to 1.381 × 10^{-16} esu^2 (cm ion K)$^{-1}$. The answer will be the same. Again, check the problem both ways to become familiar with the units used by different societies and scientists.

3.4. In the text, we stated that equation 3.17 is greatly simplified, and indicates a linear increase in potential from a charged surface when it should reflect an exponential decrease. As a result, the solution to this equation will greatly overestimate the actual potential. We shall prove that now. Assuming a parallel-plate capacitor, calculate the zeta potential 23 Å from particle surface. Using an meq density of 1.5 × 10^{-7} meq/cm^2, multiplying by 0.001N_A and by e (4.8 × 10^{-10} esu), the charge density is about 43,200 esu/cm^2. Using this value in equation 3.17, ζ_{mont} = [(4π)(43,200 esu · cm^{-2})(23 × 10^{-8} cm)/(80 esu^2 erg^{-1} cm^{-1})] = 0.0016 erg/esu, where the subscript "mont" represent

montmorillonite. Since one esu is 300 V practical, the potential is 0.468 V or 468 mV. This is a very high value and makes little sense. Now, we solve the problem in terms of ψ_0, which may be determined using the inverse sinh relation (as applied in equation 3.15) if a bulk fluid ion concentration is assumed. Assuming a 0.001 NaCl solution, ψ_0 is about 250 mV, confirming the results of van Olphen (1963, p. 255); this is substantially less than the streaming potential computed using equation 3.17, and there is no way that ζ can exceed ψ_0. Generally, the distance from the particle surface to the slipping plane is not known, although one gets the impression from van Olphen (1963) that it might be approximately (although clearly not *exactly*) $1/\kappa$. Perhaps, noting that (based on the Guoy theory) the potential at that distance is about $1/e$, or about 0.37 of that at the particle surface, it might make sense to say that, in the absence of data on electrophoresis or electroosmosis, ζ is very approximately $0.4\psi_0$, or for the above value, about 100 mV.

3.5. Using equation 3.10, and rounding for calculation, $\kappa^{-1} = [(80)(1.381 \times 10^{-16}\ \text{esu}^2\ \text{ion}^{-1}\ \text{cm}^{-1}\ \text{K}^{-1})(298\ \text{K})/(8\pi)(1^2)(4.803 \times 10^{-10}\ \text{esu ion}^{-1})^2(6.022 \times 10^{18}\ \text{ions cm}^{-3})]^{1/2} = 3.0702 \times 10^{-7}$ cm, or 30.702 Å.

3.6. By applying electroosmosis with a voltage drop of 100 volts across the column, we generate a field of strength of 1 V/cm, or 3.33×10^{-3} erg/esu cm. Using equation 3.18, we have

$$V = \frac{\left(\frac{6.92 \times 10^{-10}\ \text{C}^2}{\text{J} \cdot \text{m}}\right)\left(\frac{0.06\ \text{J}}{\text{C}}\right)\left(\frac{100\ \text{J}}{\text{C} \cdot \text{m}}\right)}{\left(\frac{4\pi 0.001\ \text{J} \cdot \text{s}}{\text{m}^3}\right)} = 3.32 \times 10^{-7}\ \text{m/s}$$

However, in practice, the volume rate of flow (electroosmotic) is measured instead of the linear velocity. Assuming the cross sectional area of a capillary is A, the volume rate of flow, $V_E = AV$. Using Ohm's law, $E = i/A\lambda'$ where I is the electric current in amps or C/s, and λ' is the specific conductance. Thus, $V_E/I = \varepsilon\zeta/4\pi\eta\lambda'$ (van Olphen 1963). Using an $\varepsilon = 78.5$ and substituting ζ and λ' we have $[(6.95 \times 10^{-10}\ \text{C}^2/\text{J})(0.06\ \text{J/C})]/[(4\pi\ 0.001\ \text{J s/m}^3)(0.1\ \text{C}^2/\text{J m s})]$, which yields $3.33 \times 10^{-8}\ \text{m}^3/\text{C}$ or $0.033\ \text{cm}^3/\text{C}$. Multiplying by I to get a water flow rate would require that I be in the range of a few to several units to be realistic.

3.7. Using equation 3.31, we obtain $P_d = \{(2)(6.02 \times 10^{18}\ \text{ions cm}^{-3})(1.381 \times 10^{-22}\ \text{atm cm}^3\ \text{K}^{-1} \cdot \text{ion}^{-1})(298\ \text{K})\} \cosh[\{(4.801 \times 10^{-10}\ \text{esu ion}^{-1})(3.336 \times 10^{-4}\ \text{erg esu}^{-1})/(1.381 \times 10^{-16}\ \text{erg ion}^{-1} \cdot \text{K}^{-1})(298\ \text{K})\} - \{1\}] = 11.65$ atm, or 1.177×10^6 Pa. This solution has used the esu system; the other constants given in the question also readily convert to the same answer obtained here in Pa. The student should work the problem both ways for comparison.

3.8. First, κ (thickness of the double layer) must be determined, using equation 3.16. To begin, we will assume $r = 5 \times 10^{-8}$ cm, $z = 1$, $\varepsilon = 80$, $n = 5 \times 10^{-3}\ \text{mol L}^{-1}$; thus, $n_0 = 3.011 \times 10^{18}\ \text{ions cm}^{-3}$ (this comes from multiplication by N_A), $k = 1.381 \times 10^{-16}\ \text{esu}^2\ (\text{ion cm K})^{-1}$, $T = 25\ ^\circ\text{C}$, $e = 4.803 \times 10^{-10}\ \text{esu ion}^{-1}$, $\psi_0 = 25$ mV ($8.339 \times 10^{-5}\ \text{erg}^{1/2}\ \text{cm}^{-1/2}$), and $H = 240 \times 10^{-8}$ cm. Substituting the required values into the equation, the inverse thickness (κ) of the double layer is $2.303 \times 10^6\ \text{cm}^{-1}$. With this value, we use equation 3.34 to calculate V_R. Hence, $V_R = \{(80)(5 \times 10^{-8}\ \text{cm})(8.339 \times 10^{-5}\ \text{erg}^{1/2}\ \text{cm}^{-1/2})^2/2\} \ln[1 + \exp\{(-2.303 \times 10^6\ \text{cm}^{-1})(240 \times 10^{-8}\ \text{cm})\}] = 5.521 \times 10^{-17}$ erg. For V_R of the platelet-shaped particle, use equation 3.32 for calculation purposes. Using the same constants as in the preceding, one should obtain 146.2 erg cm^{-2}. However, for learning purposes, calculate the problem using the following constants: $\kappa^{-1} = 30.84$ Å, $d = 150$ Å, $n_0 = 6.02 \times 10^{18}\ \text{ions cm}^{-3}$, $e = 1.6 \times 10^{-19}$ C, $\psi_0 = 75$ mV. Using these parameters, the answer in SI units is about $7.8 \times 10^{-8}\ \text{J m}^2$.

3.9. By letting $D = 2d$, the mathematical difference can be expressed as $[(1/d^3 + 1/(d + \delta)^3 - 2/\{d + \delta/2\}^3] - 1/2d^3$. If $\delta >> d$, the above expression reduces to $1/d^3 - 1/2d^3 = 1/2d^3$. Therefore, equation 3.44 produces a result that is approximately twice that of equation 3.45. For example, let $A = 1$, $d = 4 \times 10^{-10}$, $\delta = 200$, and $D = 2d$; substitution into equation 3.44 yields 2.1×10^{26} and substitution into equation 3.45 yields 1.04×10^{26}. In the case of a spherical particle, we will let $H = d, a = \delta$, and $s = \{(H/a) + 2\}$; substituting these into equation 3.46 yields 4.166×10^{10}. The value for the spherical particle is substantially less than those obtained for platelet shapes (from chapter 2, we can clearly see that this is related to specific surface

area). Additionally, forces decay much slower in the spherical case, as the value for "H" decreases. For large distances between spheres, the attractive force decays proportionally to $1/R^6$. This is similar to the case of the platelets, and is a feature of the long-range character of the van der Waals–London forces.

3.10. First, we will assume some parameter values for calculation purposes: $\sigma = 1.261 \times 10^4$ esu cm^{-2} or 3.78×10^6 V cm^{-1}, $T = 25$ °C, $\eta = 3.1 \times 10^{-2}$ (thus, by multiplication of N_A, $\eta_0 = 1.866 \times 10^{19}$ ion cm^{-3}), $z = 1$, $k = 1.381 \times 10^{-16}$ erg (ion K)$^{-1}$ or 1.382×10^{-16} esu^2 (ion K cm)$^{-1}$, and $e = 4.803 \times 10^{-10}$ esu ion^{-1}. From this information, using equation (3.16), $\kappa = 5.8 \times 10^6$ cm^{-1}. Therefore, $\psi_0 = \{(3.78 \times 10^6 \text{ V cm}^{-1})(4\pi)\}/\{(78.3)(5.8 \times 10^6 \text{ cm}^{-1})\} = 104.6$ mV.

3.11. Using equation 3.68, $\mu_0 = -4.841 \times 10^{-4}$ atm g^{-1} cm^3 (atm per unit of water), or -490.6 erg g^{-1}.

3.12. The most laborious calculation for this problem is that of y_d from equation 3.76 (right-hand side for anions); thus, $y_d = \exp[\{(1)(4.803 \times 10^{-10} \text{ esu ion}^{-1})(4.336 \times 10^{-5} \text{ esu cm}^{-1})\}/\{(1.381 \times 10^{-16} \text{ esu}^2 \text{ ion}^{-1} \text{ K}^{-1} \text{ cm}^{-1} (298 \text{ K})\}] = 1.659$. Thus, using this value in equation 3.73, we obtain $\Delta P = [(2)(0.082 \text{ atm L mol}^{-1} \text{ K}^{-1})(298 \text{ K})(0.01 \text{ mol L}^{-1})][\cosh(1.659) - 1] = 0.841$ atm.

3.13. Use the equation $E_i = (2\Pi\sigma^2 d)/\varepsilon$. First, calculation of Π must be performed. $\Pi = MRT$; thus, given $M = 10^{-2}$ M, $R = 0.082$ atm L mol^{-1} K^{-1}, and $T = 25$ °C, $\Pi = 0.758$. Thus, $E_i = (2) \times (0.758)(1.26 \times 10^4 \text{ esu cm}^2)(2.6 \times 10^{-8} \text{ cm})/78.3 = 7.99 \times 10^{-2}$ erg cm^{-2}. Consider how this value would compare to that from other equations.

3.14. Converting units and using equation 3.77, $F_c = 18.74$ mmol L^{-1}. Novich and Ring (1984) lists a value of $A = 2.2 \times 10^{-20}$ J for montmorillonite. Recalculate the problem based on their experimental value.

3.15. The primary usefulness of BTCs is that they can reveal a great deal about a given soil: degree of aggregation, presence of macropores, adsorption sites, anion exclusion, and so on. For more details on BTCs, see chapter 10.

3.16. Environmental causes are kinetic energy due to raindrop impact, freezing and thawing, and rapid wetting of dry materials. These effects are greatly exacerbated when the soil is wet.

3.17. Several examples are infiltration, erosivity, particle size distribution, and profile development. Using infiltration as an example, as long as a clay is flocculated, there will be significantly greater infiltration. If the media starts to disperse, the smaller clay particles will clog surface pores and reduce infiltration.

ADDITIONAL QUESTIONS

3.18. What is the primary binding force between adsorbed cations and a clay platelet?

3.19. What is the difference in electrostatic attraction by a clay platelet to Na^+ ions and Ca^{2+} ions?

3.20. How does the electrostatic attractive force change, qualitatively, with distance from a clay platelet?

3.21. What is the electrical status of a clay platelet dried out from a soil solution?

3.22. What will be the influence of salt concentration in the bulk solution on the extent of the double layer?

3.23. Suppose the cations in the double layer are Na^+ ions, and that they are then replaced by an ionic equivalent of Ca^{2+} ions. Describe, quantitatively, how the equilibrium distribution of ionic equivalents in the diffuse layer will change. Use a sketch.

3.24. **(a)** As a scientist, you would like to know how thick the water film might be around clay platelets that are air dry. Assume air-dry $w = 0.21$ g/g and $a_m = 132.3$ m^2/g. Ignore any water that remains after oven drying (105 °C/24 hr). Express your answer in Å.

(b) How many water molecules thick is this layer.

3.25. Why is the osmotic pressure in the double layer higher for a clay containing sodium than for a clay containing calcium?

3.26. How is the stability of plate condensation influenced by the amount of salts in soil water?

3.27. Explain how plate condensation and cardhouse-type flocculation take place in clay suspensions. ("Cardhouse flocculation": Some charged surfaces such as the edges of clay and surfaces of sesquioxides can become positively charged under acid conditions, which results in coulombic interaction between particles. This leads to a type of edge-to-face flocculation at low electrolyte concentrations in which the attraction of particles resembles a house of cards. This is also referred to as mutual flocculation.)

3.28. A soil aggregate with a mass of 8.99 g, sealed in wax, is lowered into a container of water on a string attached to a torsion balance. At equilibrium, the balance reads 2.79 g. Assume the mass of wax and string are negligible.

(a) Calculate the weight of the aggregate.

(b) What is the dry bulk density of the aggregate?

3.29. **(a)** Calculate the CEC in meq/100g soil for the following.

montmorillonite	$(Si_g)^{IV}(Al_{3.5}Mg_{0.5})^{VI}O_{20}(OH)_4$
illite	$(Si_7Al_1)^{IV}(Al_4)^{VI}O_{20}(OH)_4K_{0.8}$
vermiculite	$(Si_6Al_2)^{IV}(Al_4)^{VI}O_{20}(OH)_4K_{0.5}$

(b) What ions have substituted for what other ion, and did this substitution take place in the octahedral or tetrahedral layer?

3.30. By an examination of the capillary rise phenomena, the total energy (E) associated with both interfaces (air and water) is

$$E = \sigma f + \gamma i = \sigma s/\sin\phi + \gamma s/\tan\phi$$

where σ is surface tension (J m^{-2}), which is the interface potential energy divided by interface area; and γ is the potential energy of water molecules near the solid surface, divided by the area of the solid–water interface (J m^{-2}). The angle (ϕ) will adjust itself until E is at a minimum. Describe this mathematically.